Topology and interactions within the magic angle twisted bilayer graphene narrow bands

Oskar Vafek

National High Magnetic Field Laboratory

and

Department of Physics, Florida State University, Tallahassee, FL

The role of symmetry in TBG band topology

- In general, the $C_{2z}T$ symmetry requires $\det W(k_2) = \pm 1$

$\det W(k_2) = +1$	$\det W(k_2) = -1$
• the two eigenvalues are complex conjugates of each other	• the two eigenvalues are real and (1,-1) independent of k_2 (i.e. trivial winding) (we find this in the $C_{2z}T$ symmetric period-2 stripe state)

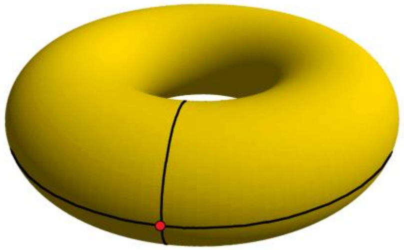

Fang Xie, Zhida Song, Biao Lian, and B. Andrei Bernevig PRL 124, 167002 (2020)
Fang Xie, Jian Kang, B Andrei Bernevig, OV, Nicolas Regnault arXiv:2209.14322

Recall: $\boldsymbol{B} = 0$ narrow band hybrid Wannier states of the non-interacting model

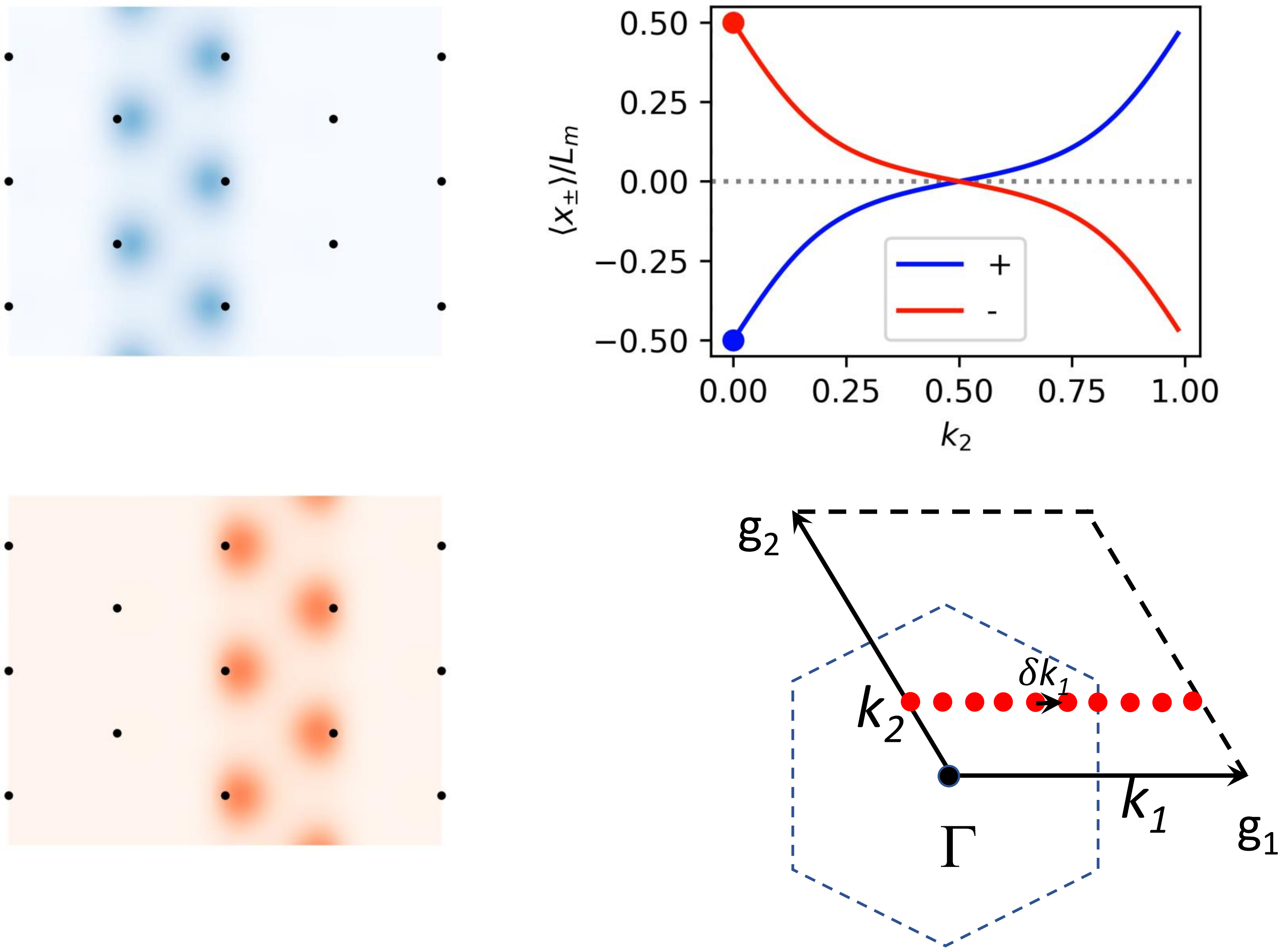

(iTensor) DMRG results

(spinless one valley)

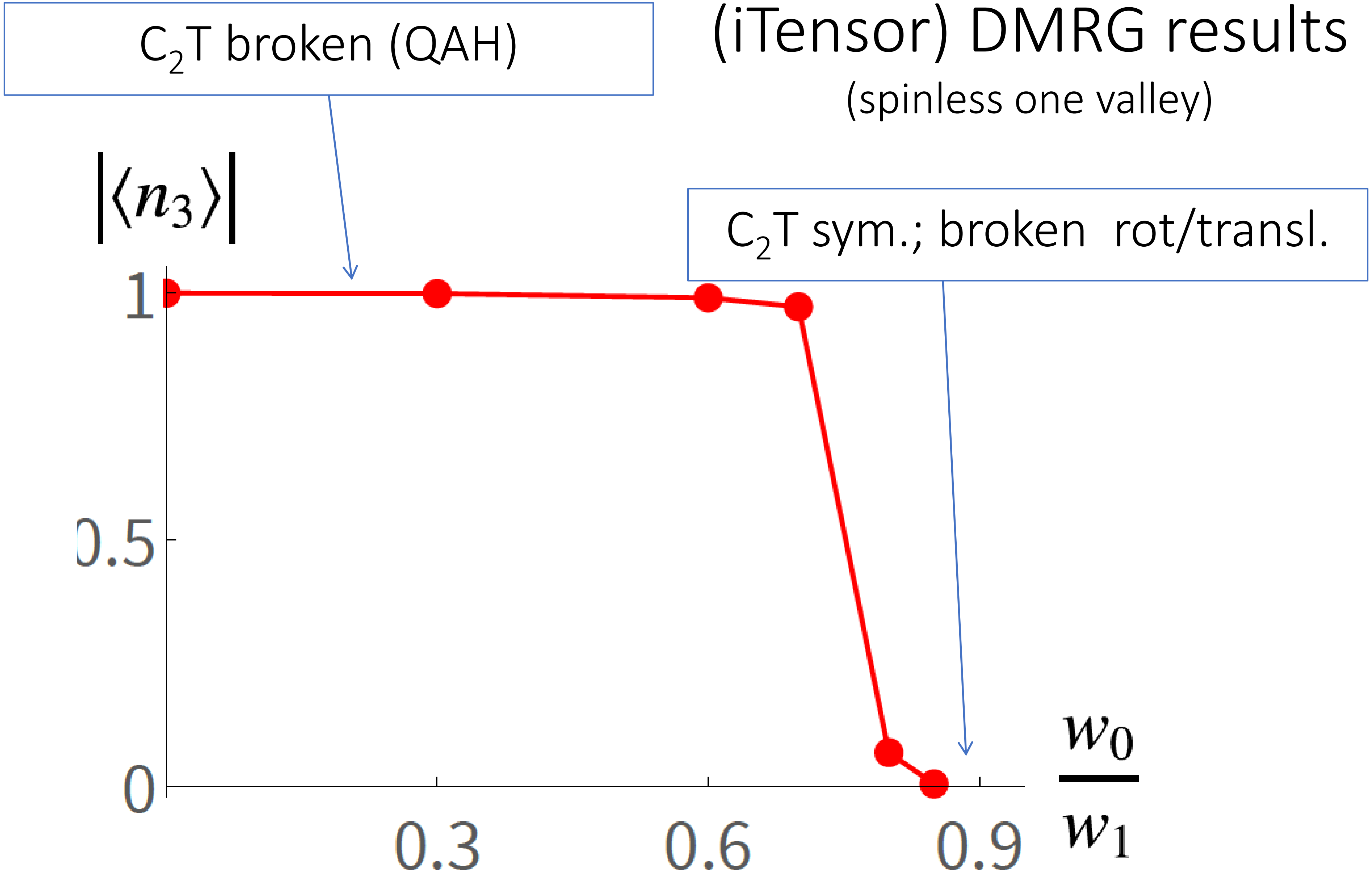

J. Kang and OV, PRB 2020

(iTensor) DMRG results: almost exclusively single occupancy

(n,k)	$(0,\frac{1}{12})$	$(0,\frac{1}{4})$	$(0,\frac{5}{12})$	$(0,\frac{7}{12})$	$(0,\frac{3}{4})$	$(0,\frac{11}{12})$
$P(\hat{N}_{n,k}=0)$	0.038	0.017	0.018	0.018	0.018	0.036
$P(\hat{N}_{n,k}=1)$	0.922	0.966	0.965	0.964	0.965	0.924
$P(\hat{N}_{n,k}=2)$	0.040	0.017	0.017	0.018	0.017	0.040

J. Kang and OV, PRB 102, 035161 (2020)

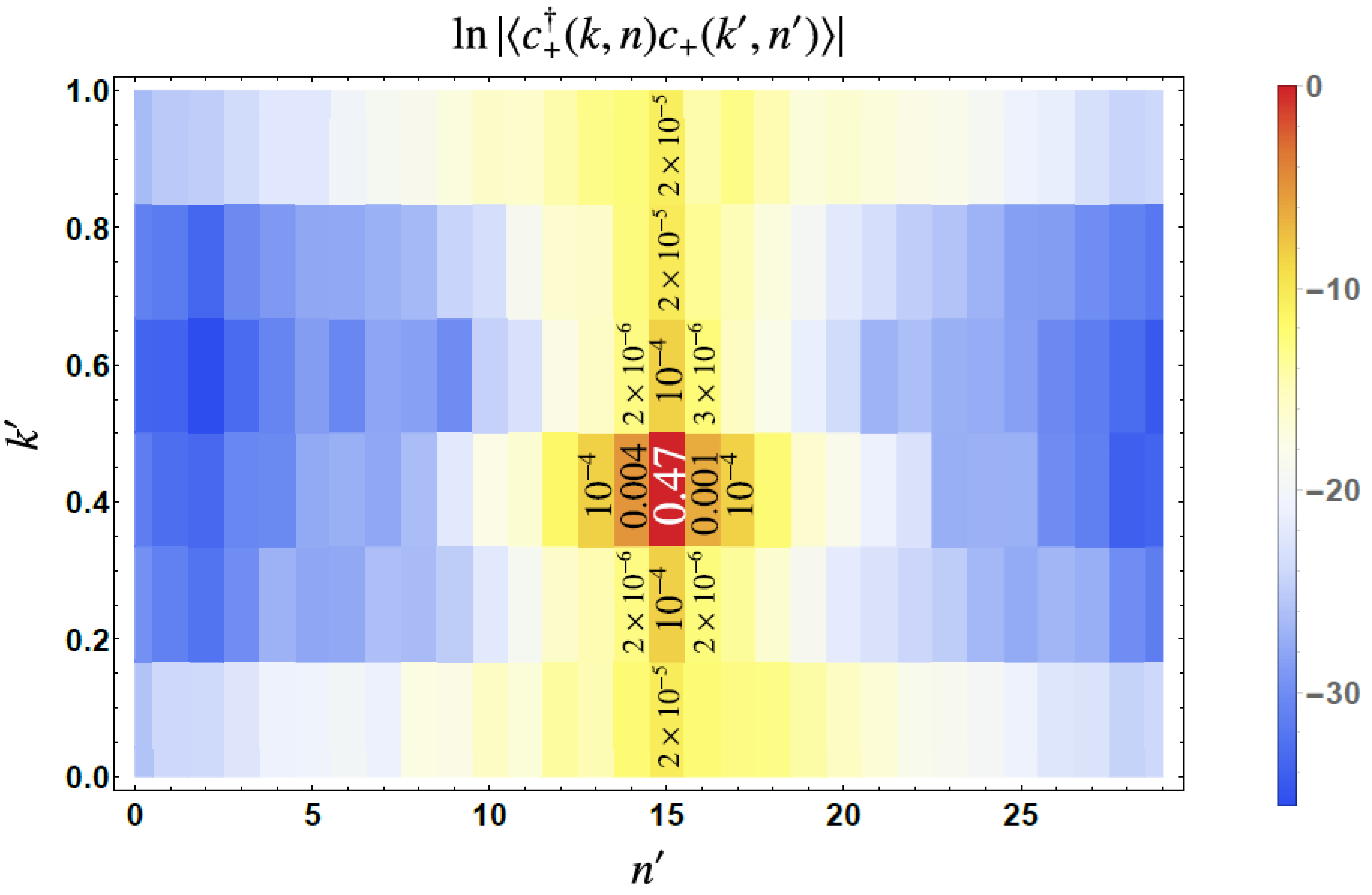

J. Kang and OV arXiv:2002.10360

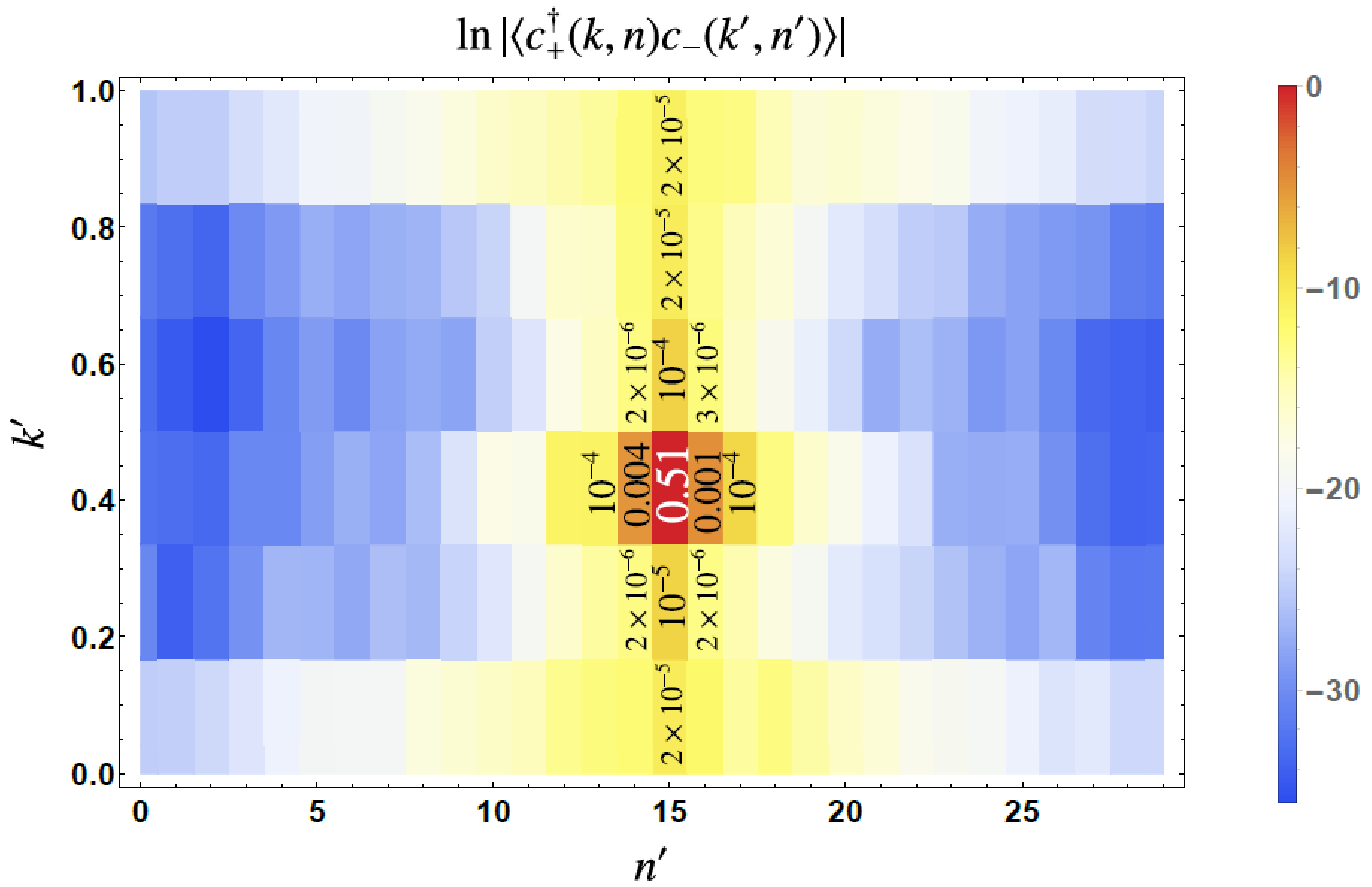

J. Kang and OV, PRB 102, 035161 (2020)

Subsequently confirmed by a more accurate DMRG algorithm (Zaletel's group)

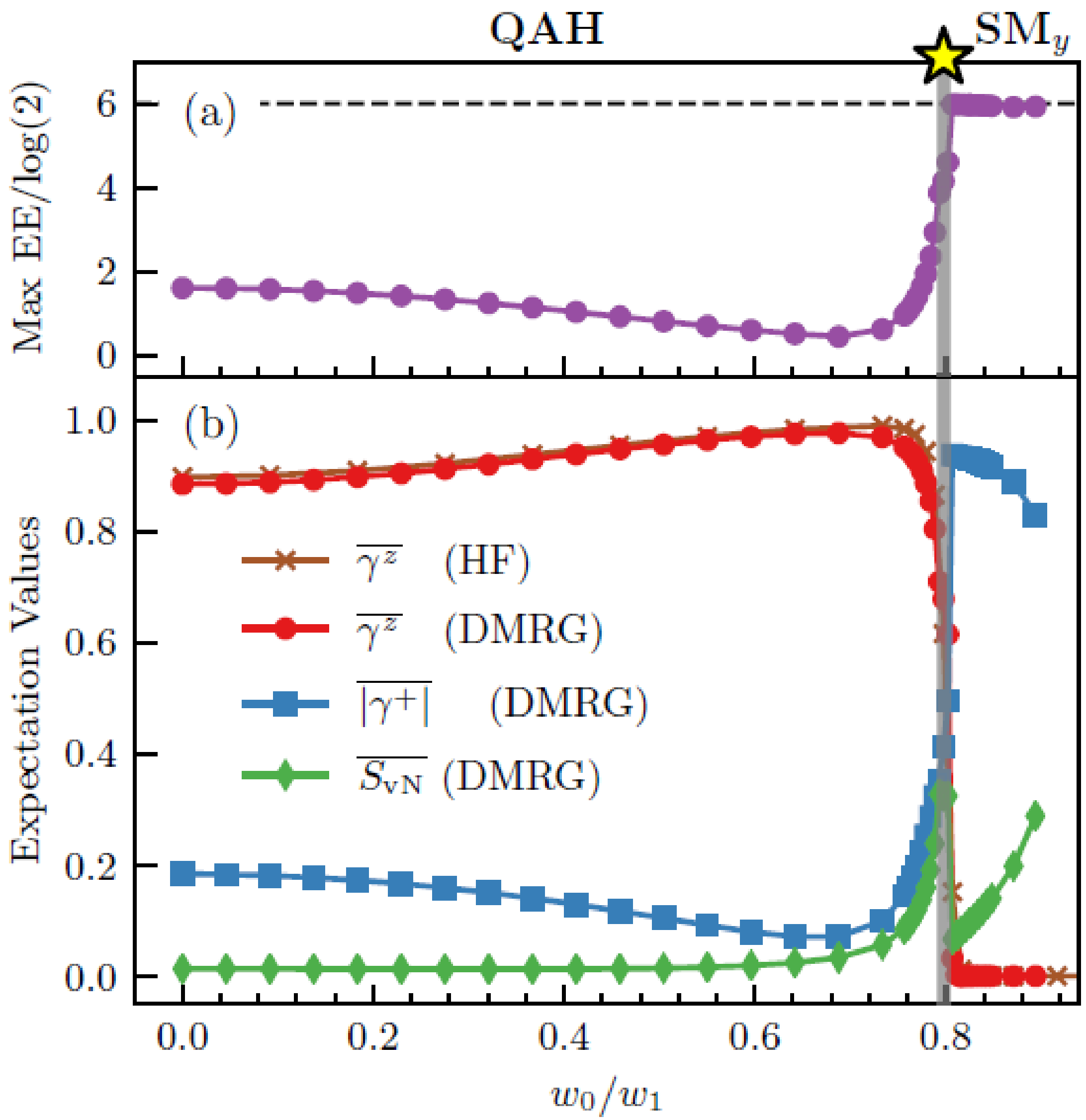

Soejima et al Phys. Rev. B 102, 205111 (2020)

Energetics from a more accurate DMRG algorithm N_y=6 (Zaletel's group)

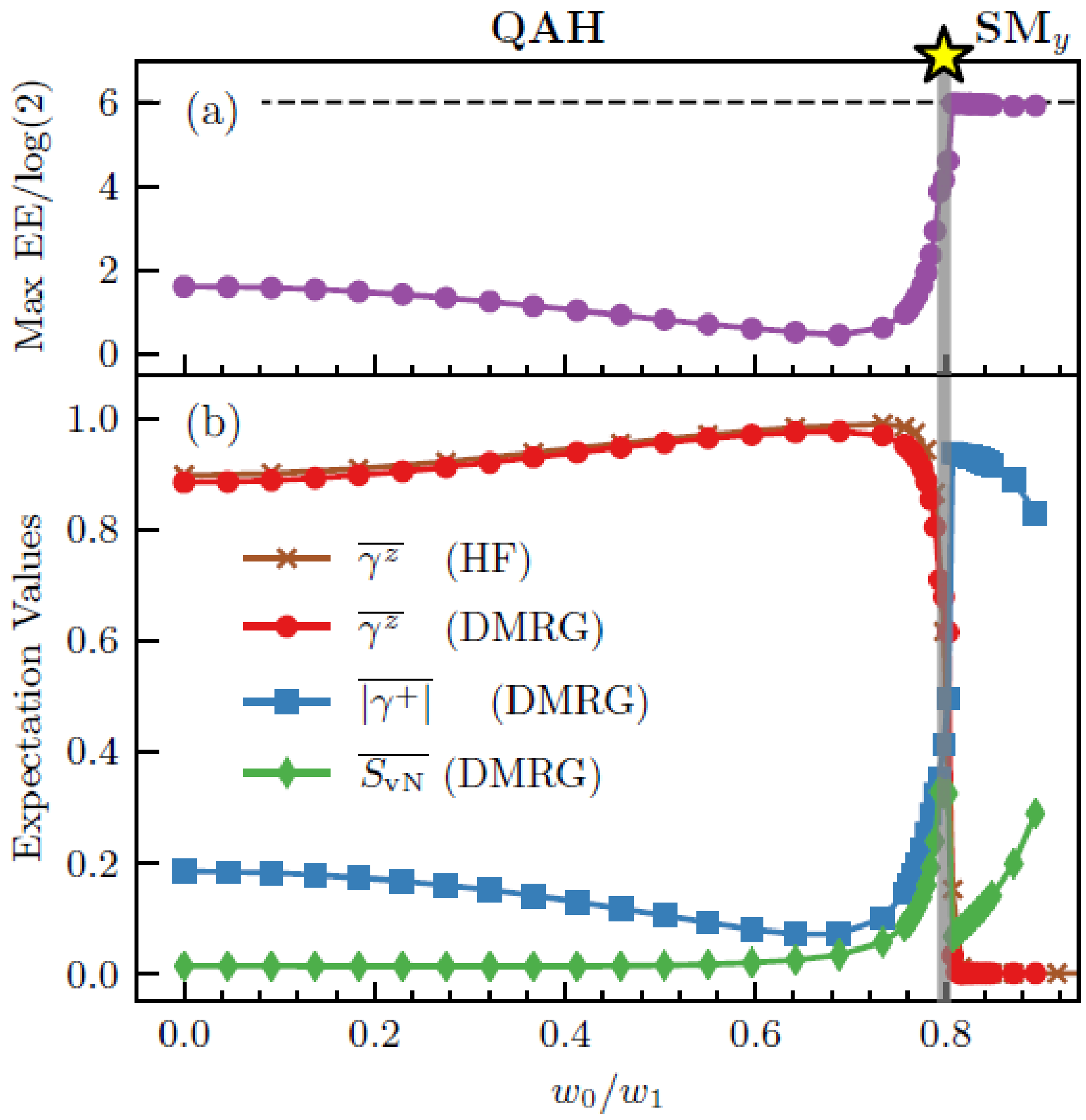

State	Energy (meV)
DMRG ground state (SM_y)	−28.24
QAH ansatz [Eq. (14)]	−28.04
SM_y ansatz [Eq. (14)]	−27.92
$C_2\mathcal{T}$ - stripe ansatz [Eq. (14)]	−28.08
Dirac (BM ground state)	−20.62

Soejima et al Phys. Rev. B 102, 205111 (2020)

$\upsilon = -3$ for ${}^{w_0}/_{w_1} \neq 0$

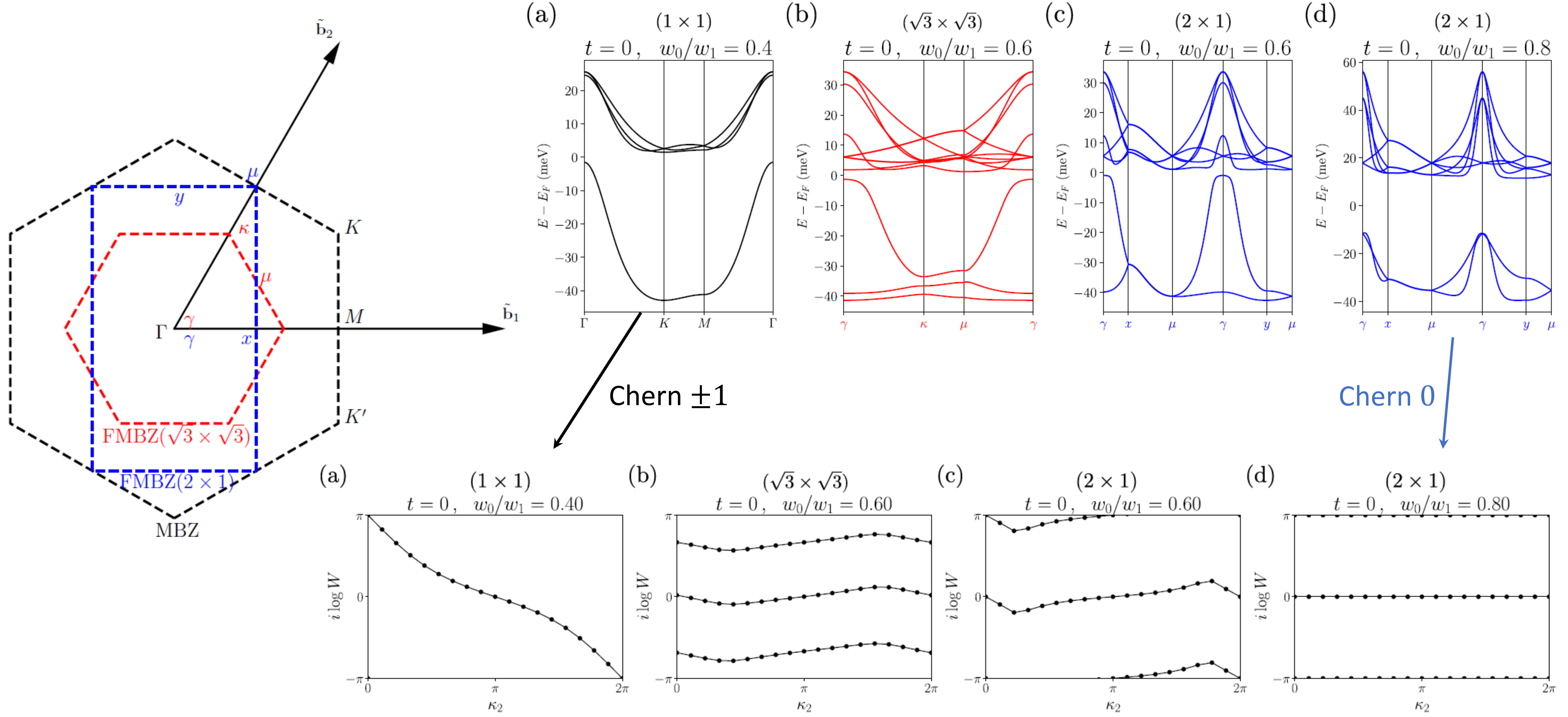

Fang Xie, Jian Kang, B Andrei Bernevig, OV, Nicolas Regnault arXiv:2209.14322

Odd filling for $w_0/w_1 \neq 0$

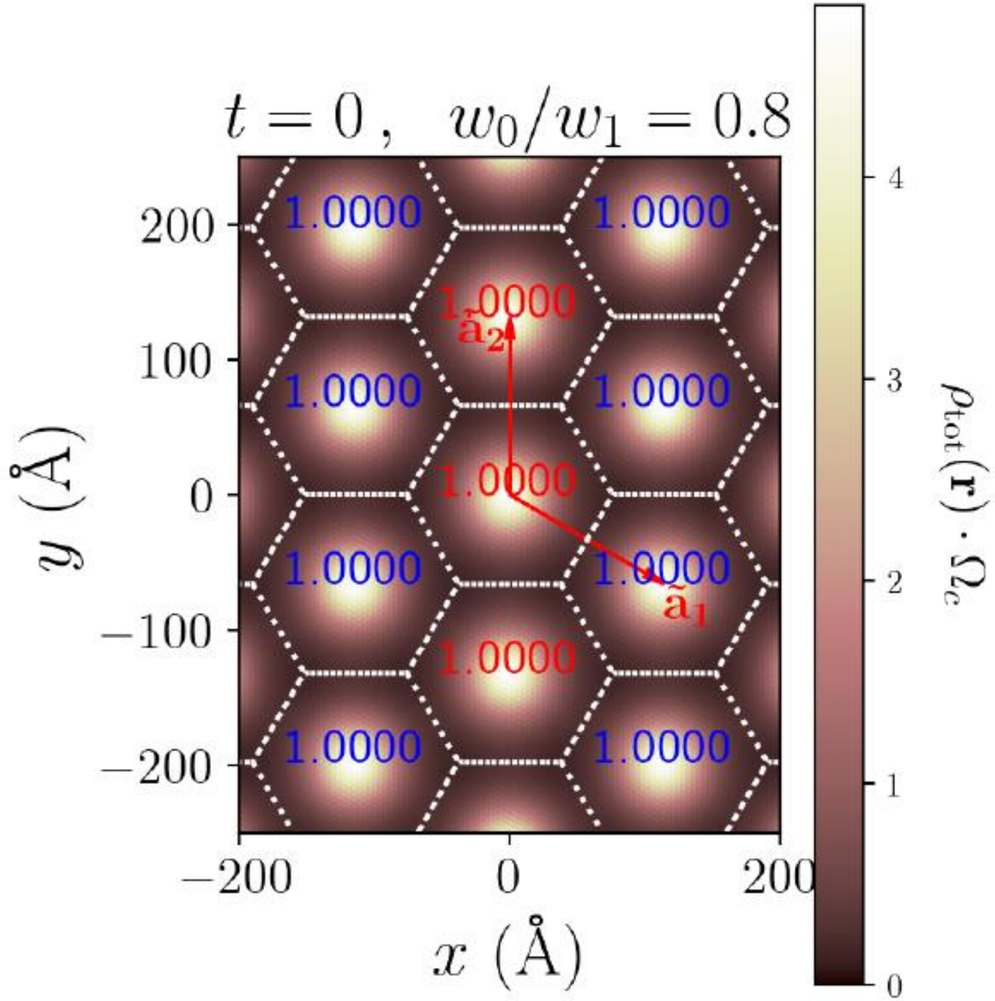

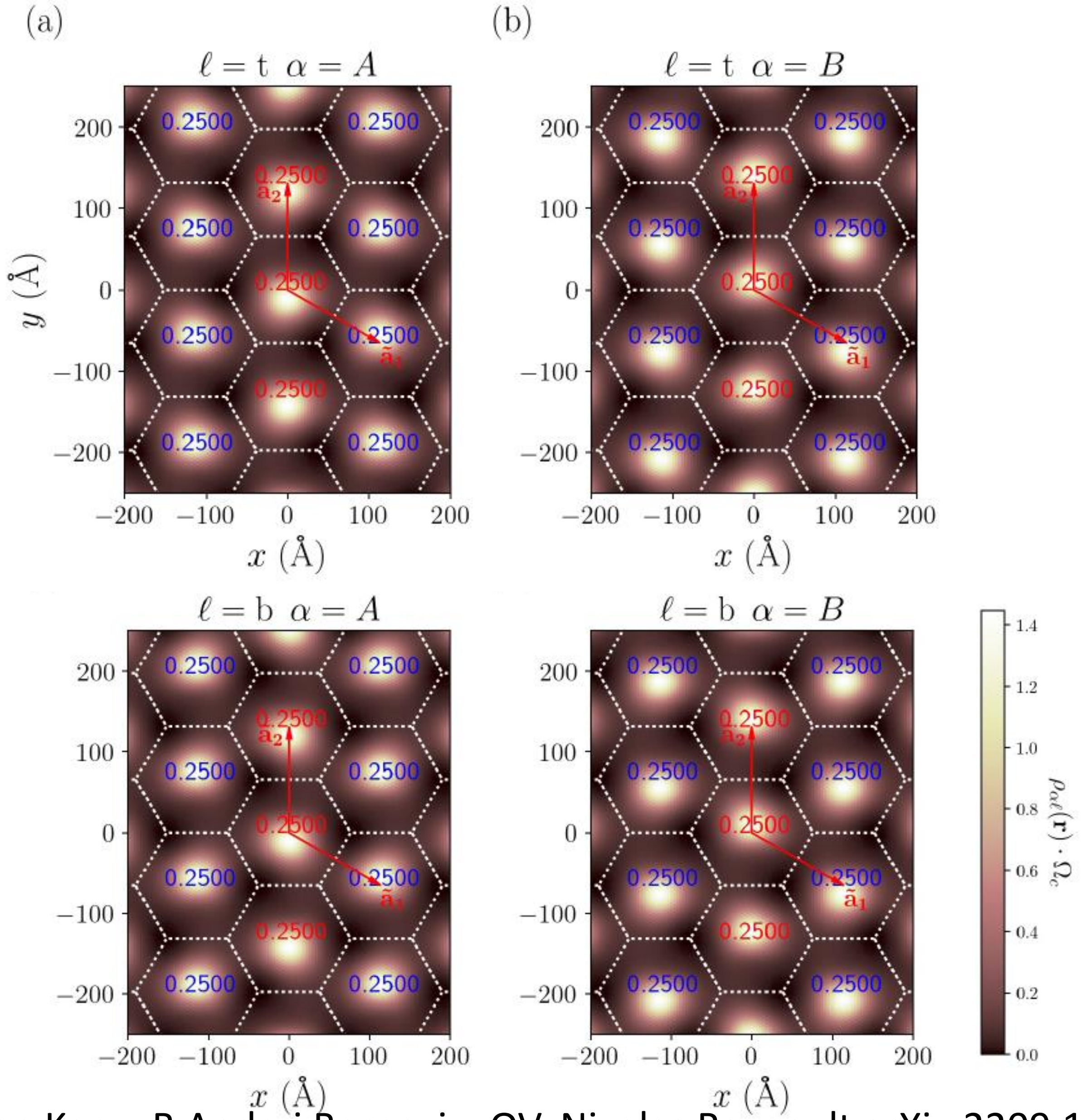

Fang Xie, Jian Kang, B Andrei Bernevig, OV, Nicolas Regnault arXiv:2209.14322

Lecture 2:

- $B \neq 0$ Interacting Hofstadter spectrum at strong coupling of twisted bilayer graphene

- Outlook: Near degeneracy among many phases and strong sensitivity to strain motivated development of a more accurate continuum model than the minimal

    from microscopic model to continuum theory via systematic gradient expansion

    comparison of the structure with data

Exact single particle excitation spectrum at integer filling in the strong coupling

$$\left(E - E_v^{(0)}\right) X|\Omega_v\rangle$$

$$= \frac{1}{2}\int d\boldsymbol{r}\, d\boldsymbol{r}' V(\boldsymbol{r} - \boldsymbol{r}')\big[\delta\varrho(\boldsymbol{r}), [\delta\varrho(\boldsymbol{r}'), X]\big]|\Omega_v\rangle + \int d\boldsymbol{r}\, d\boldsymbol{r}' V(\boldsymbol{r} - \boldsymbol{r}')[\delta\varrho(\boldsymbol{r}), X\,]\delta\bar{\varrho}_v(\boldsymbol{r}')|\Omega_v\rangle$$

$\mathcal{E}^{(F)}(\boldsymbol{k})$

$\pm\mathcal{E}_\nu^{(H)}(\boldsymbol{k})$

Hofstadter spectra at strong coupling

Xiaoyu Wang

We need to find a projector onto the narrow bands at finite B-field

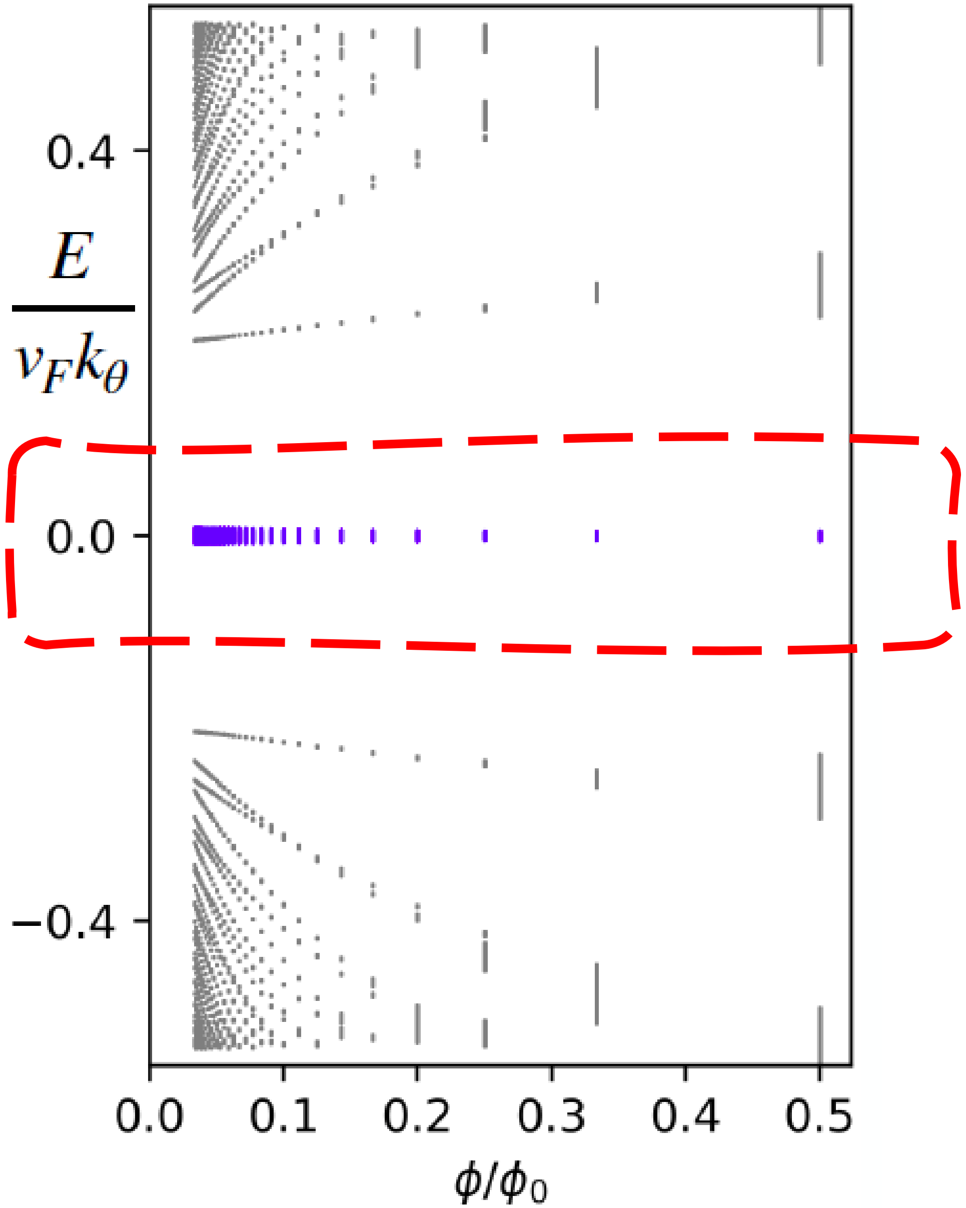

$$V_{int} = \frac{1}{2}\int d\boldsymbol{r}d\boldsymbol{r}'\, V(\boldsymbol{r}-\boldsymbol{r}')\delta\rho(\boldsymbol{r})\delta\rho(\boldsymbol{r}')$$

- One option is to solve the BM model in LL basis
- Problematic at low **B** and near simple fractions because of the high number of LLs that needs to be kept
- Need a new method (that works even if the narrow bands are topological at **B**=0)

X. Wang and OV arXiv:2112.08620

Recall: $\boldsymbol{B} = 0$ narrow band hybrid Wannier states of the non-interacting model

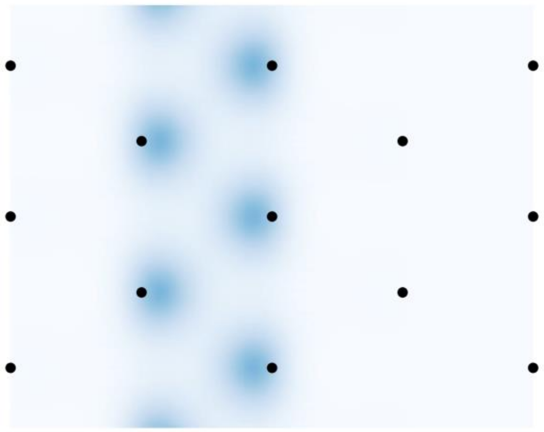

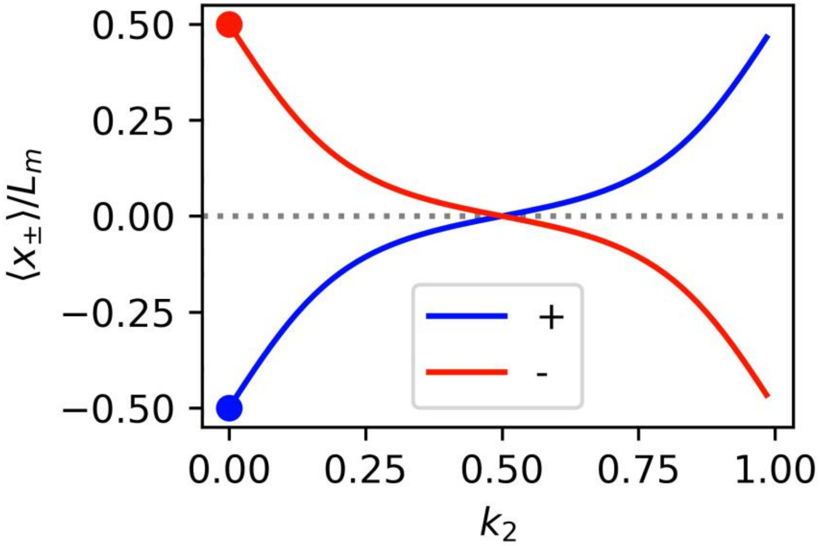

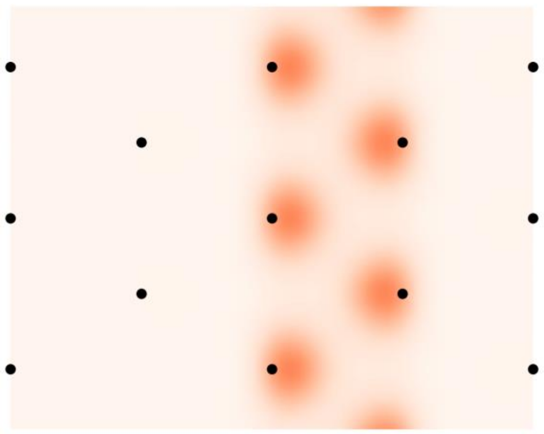

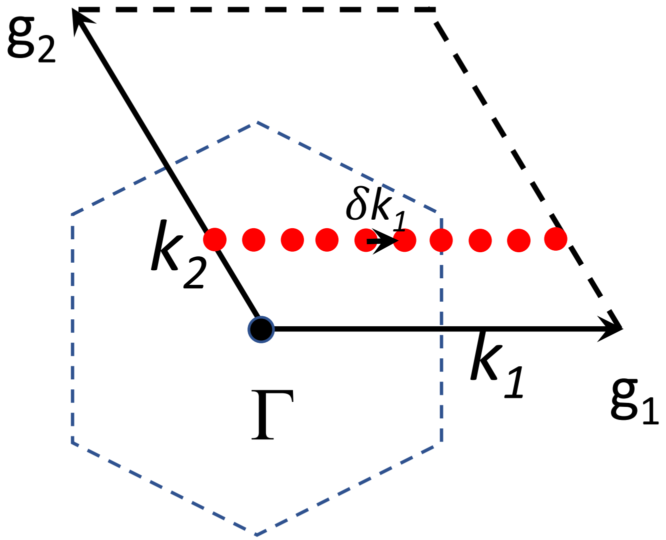

Key insight

- for the hybrid Wannier state centered at and near the origin, the Landau gauge vector potential $\boldsymbol{A} = (0, Bx)$ can be treated perturbatively, because the region in real space where $\boldsymbol{A}$ is large gets suppressed by the exponential localization of the hybrid Wannier state.
- the discrete translation symmetry along the y −direction used in constructing the hybrid Wannier state is preserved by such $\boldsymbol{A}$
- Generate the entire basis from the **B**=0 hybrid WS centered near origin by projecting onto irreps of MTG

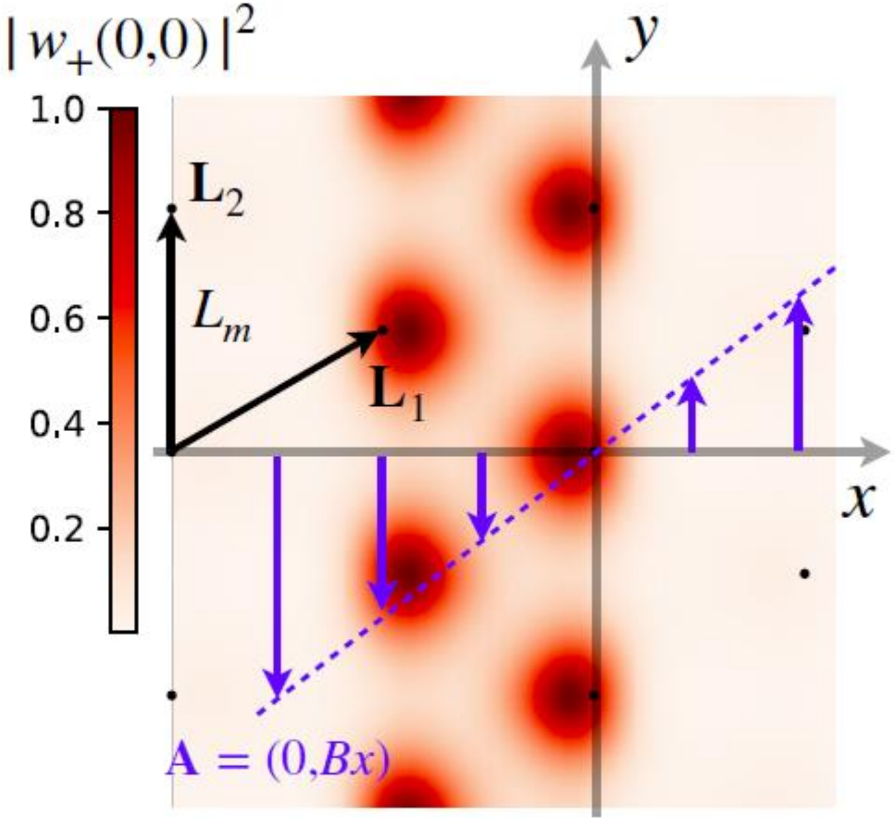

Xiaoyu Wang and OV PRB, 106, L121111 (2022)

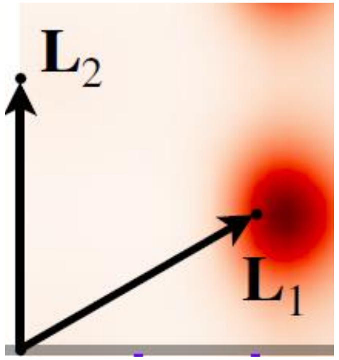

$$t_{\boldsymbol{L}_2}\psi(\boldsymbol{r}) = \psi(\boldsymbol{r}-\boldsymbol{L}_2)$$

$$t_{\boldsymbol{L}_1}\psi(\boldsymbol{r}) = e^{i\frac{eB}{\hbar c}L_{1x}y}\psi(\boldsymbol{r}-\boldsymbol{L}_1)$$

$$\frac{\phi}{\phi_0} = \frac{p}{q}$$

$$\left[t_{\boldsymbol{L_2}}, H_{BM}\left(p_x, p_y - \frac{e}{c}Bx\right)\right] = 0$$

$$\left[t_{\boldsymbol{L_1}}, H_{BM}\left(p_x, p_y - \frac{e}{c}Bx\right)\right] = 0$$

$$\left[t_{\boldsymbol{L_2}}^{q}, t_{\boldsymbol{L_1}}\right] = 0$$

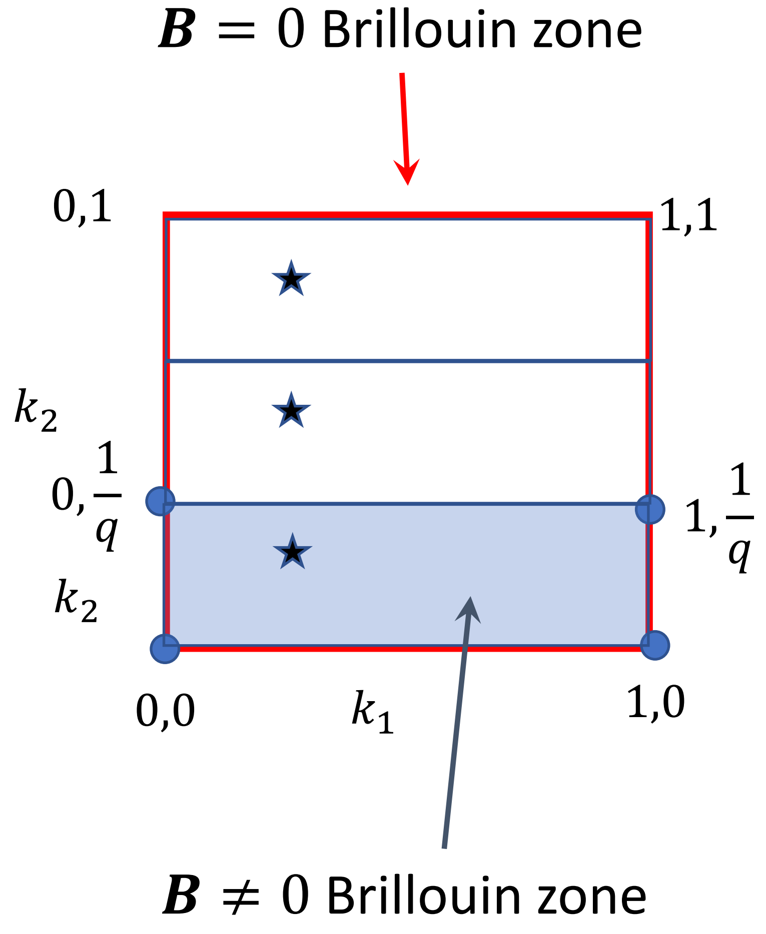

$$\boxed{|W_{\pm}(k_1,k_2;n_0)\rangle \sim \sum_{s=-\infty}^{\infty} t_{\boldsymbol{L}_1}^{s}\, e^{2\pi i s k_1}|w_{\pm}(n_0,k_2\boldsymbol{g}_2)\rangle}$$

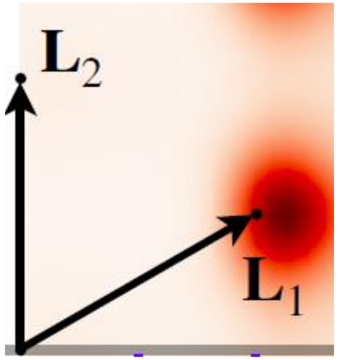

$$t_{\boldsymbol{L}_2}\psi(\boldsymbol{r}) = \psi(\boldsymbol{r}-\boldsymbol{L}_2)$$

$$t_{\boldsymbol{L}_1}\psi(\boldsymbol{r}) = e^{i\frac{eB}{\hbar c}L_{1x}y}\psi(\boldsymbol{r}-\boldsymbol{L}_1)$$

$$\frac{\phi}{\phi_0} = \frac{p}{q}$$

$$\left[t_{\boldsymbol{L_2}}, H_{BM}\left(p_x, p_y - \frac{e}{c}Bx\right)\right] = 0$$

$$\left[t_{\boldsymbol{L_1}}, H_{BM}\left(p_x, p_y - \frac{e}{c}Bx\right)\right] = 0$$

$$\left[t_{\boldsymbol{L_2}}^q, t_{\boldsymbol{L_1}}\right] = 0$$

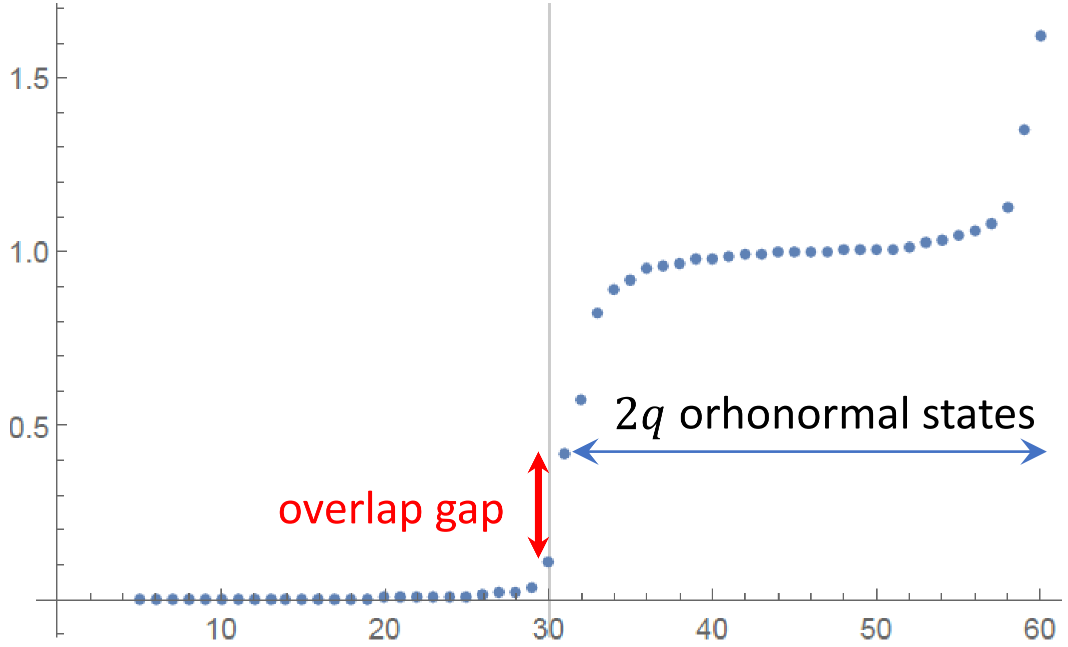

$$\boxed{|W_\pm(k_1,k_2;n_0)\rangle \sim \sum_{s=-\infty}^{\infty} t_{\boldsymbol{L}_1}^s\, e^{2\pi i s k_1}|w_\pm(n_0,k_2\boldsymbol{g}_2)\rangle}$$

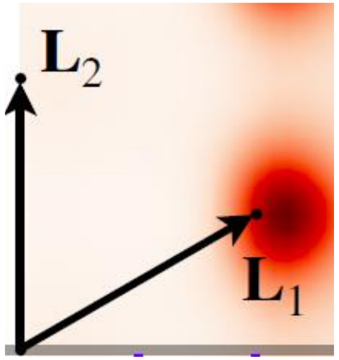

$$t_{\boldsymbol{L}_2}\psi(\boldsymbol{r}) = \psi(\boldsymbol{r}-\boldsymbol{L}_2)$$

$$t_{\boldsymbol{L}_1}\psi(\boldsymbol{r}) = e^{i\frac{eB}{\hbar c}L_{1x}y}\psi(\boldsymbol{r}-\boldsymbol{L}_1)$$

$$\frac{\phi}{\phi_0} = \frac{p}{q}$$

$$\left[t_{\boldsymbol{L_2}}, H_{BM}\left(p_x, p_y - \frac{e}{c}Bx\right)\right] = 0$$

$$\left[t_{\boldsymbol{L_1}}, H_{BM}\left(p_x, p_y - \frac{e}{c}Bx\right)\right] = 0$$

$$\left[t_{\boldsymbol{L_2}}^q, t_{\boldsymbol{L_1}}\right] = 0$$

$$\boxed{|W_{\pm}(k_1,k_2;n_0)\rangle \sim \sum_{s=-\infty}^{\infty} t_{\boldsymbol{L}_1}^s\, e^{2\pi i s k_1}|w_{\pm}(n_0,k_2\boldsymbol{g}_2)\rangle}$$

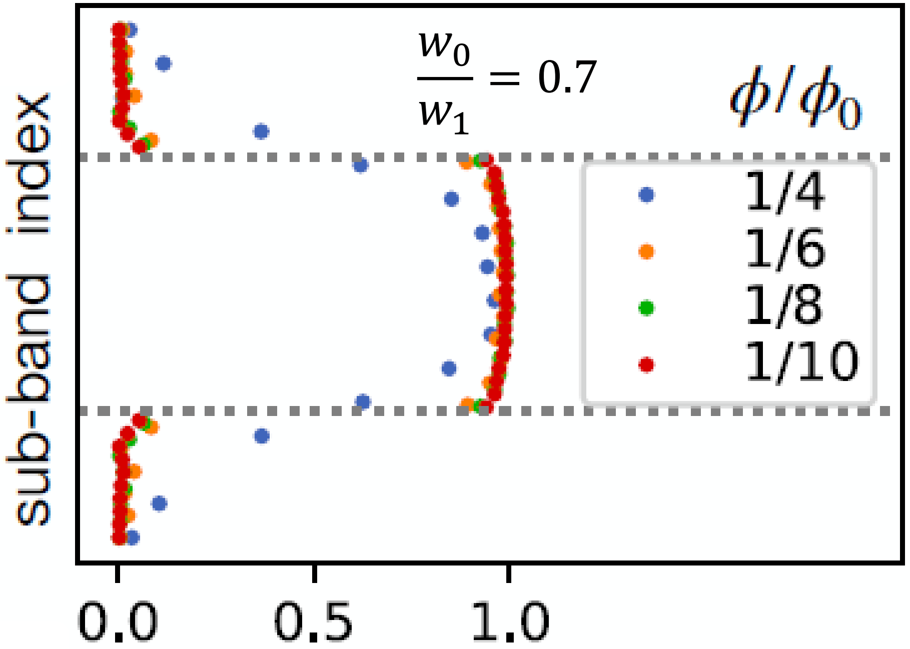

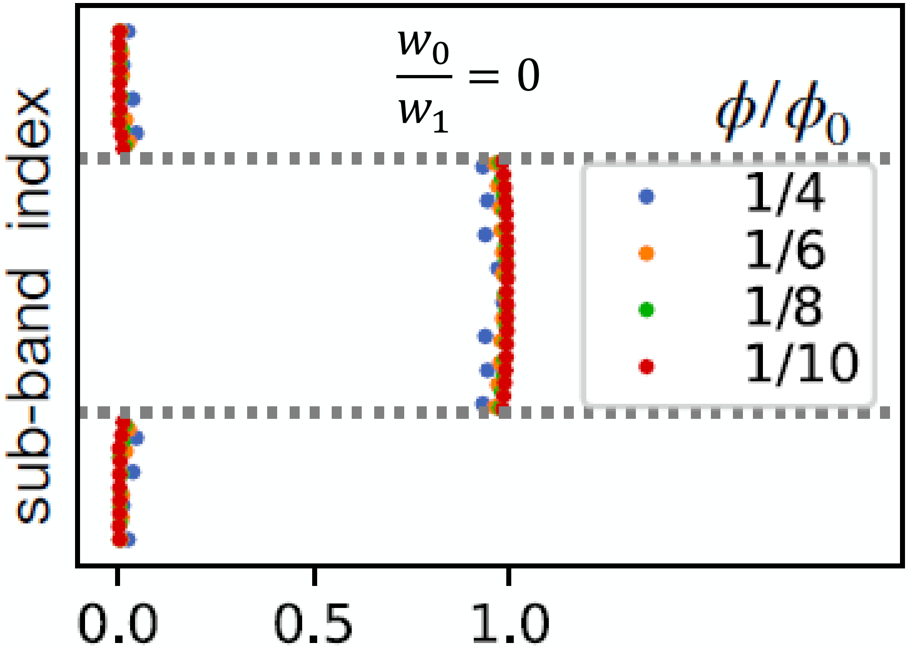

Comparison of the non-interacting Hofstadter spectrum based on hybrid Wannier states method and based on the LL method

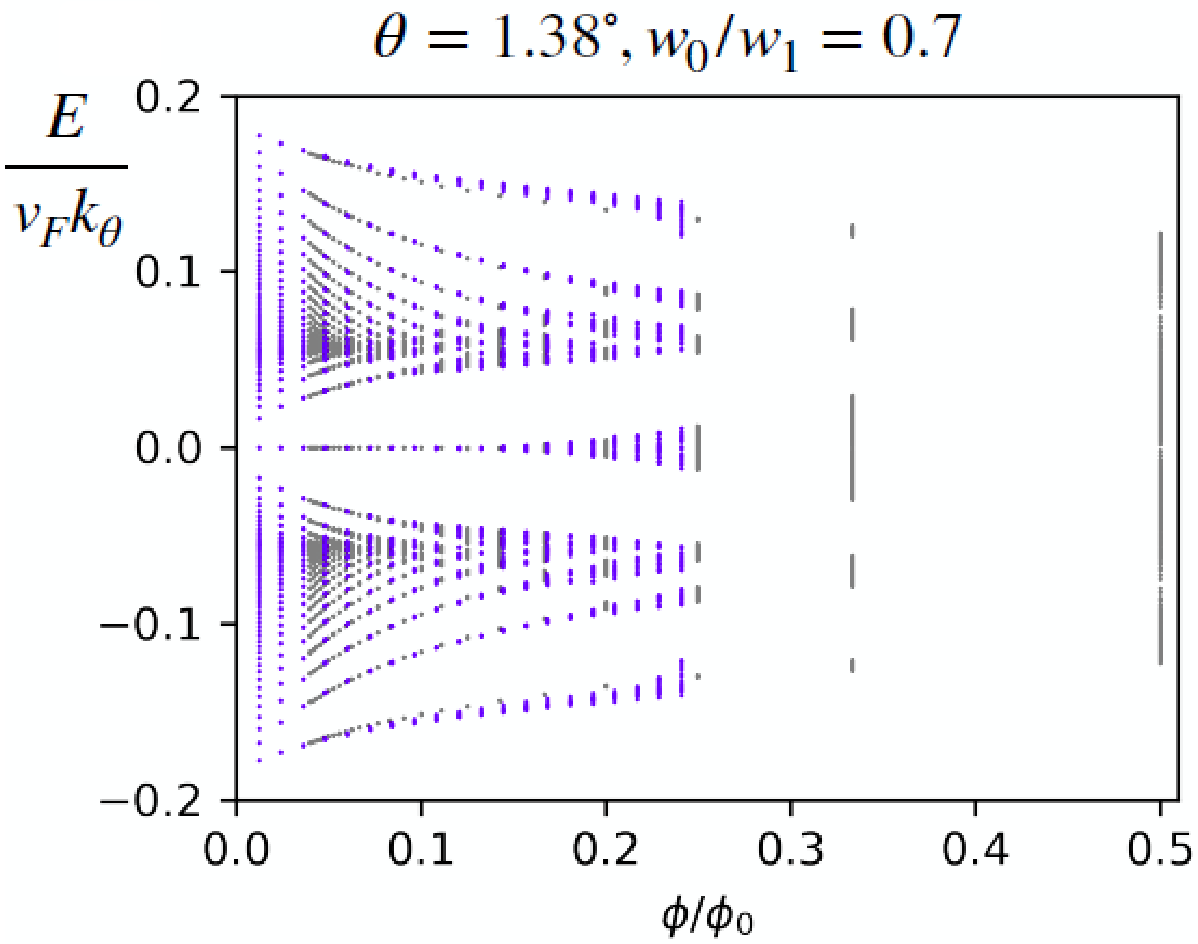

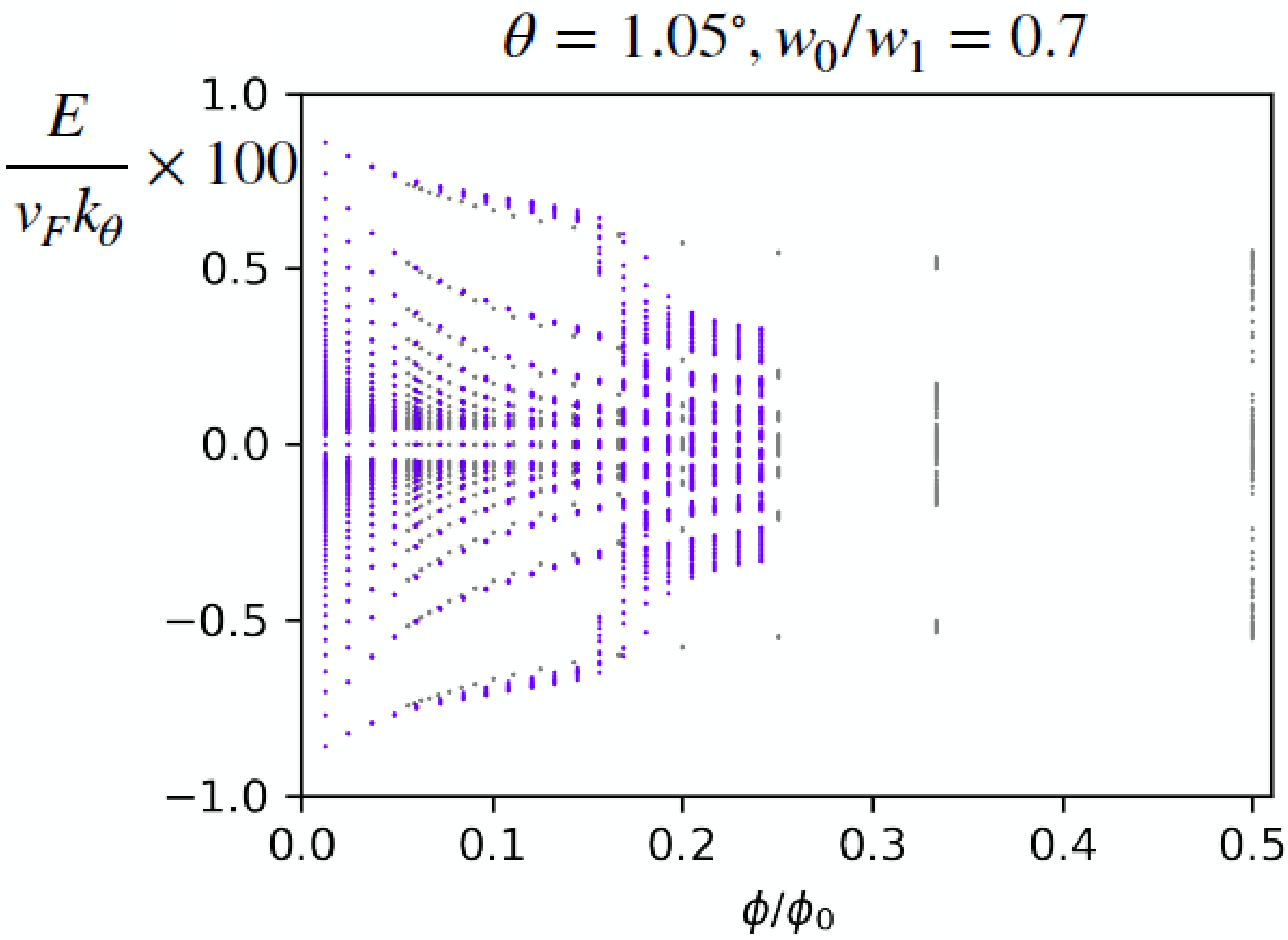

Xiaoyu Wang and OV PRB, 106, L121111 (2022) (SI)

Exact single particle excitation spectrum at CNP in the strong coupling limit at small B-field

$$V_{int}\,X|\Omega\rangle = \frac{1}{2}\int dr\,dr' V(r-r')\big[\delta\varrho(r),[\delta\varrho(r'),X]\big]|\Omega\rangle$$

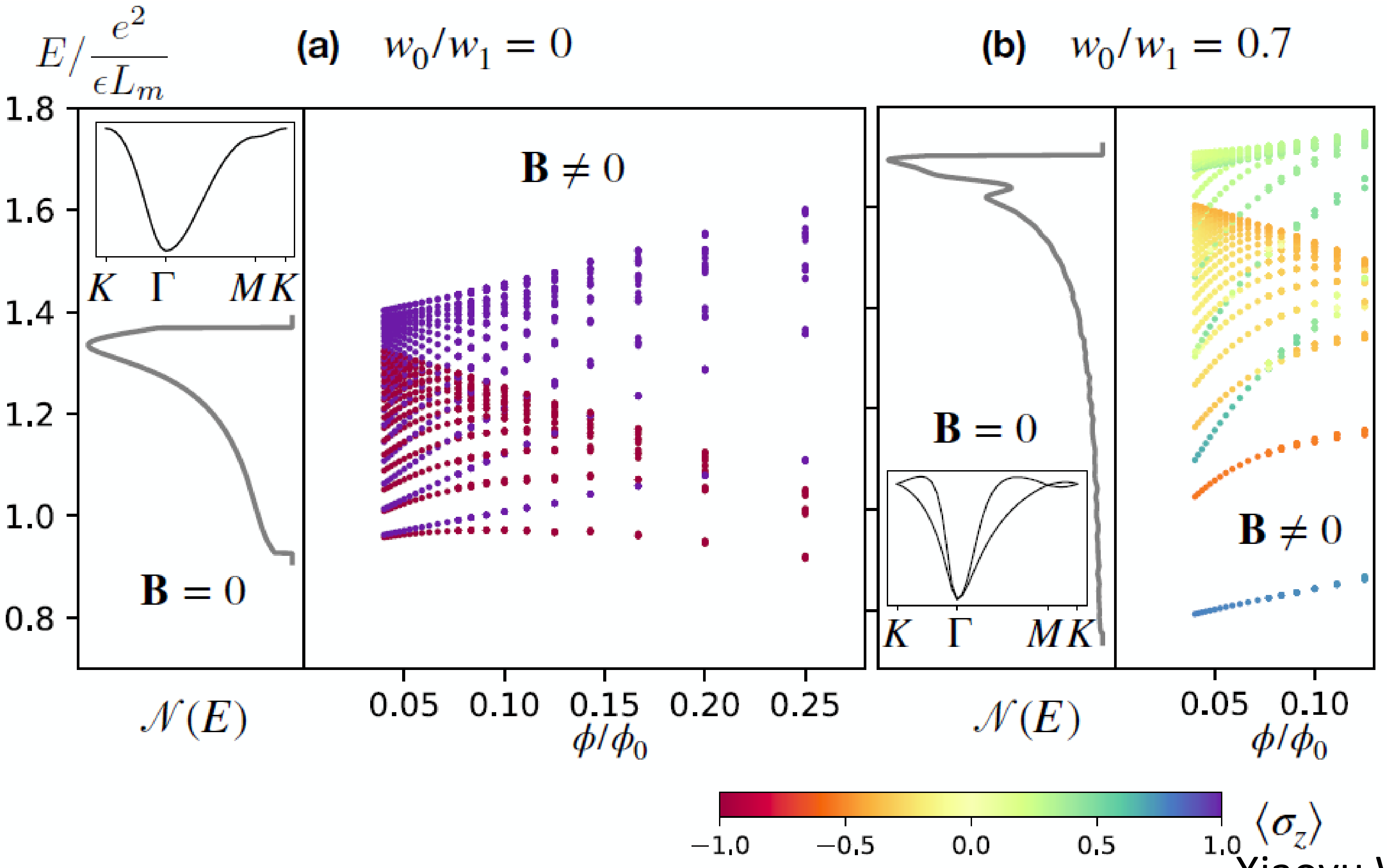

- Landau quantization even in strong coupling
- Imbalance in the sublattice polarization reflects the topology of the bands (blue is subl. A)
- Finite **B**-field causes splitting between the LLs even in the chiral limit due to broken C_2T

Xiaoyu Wang and OV PRB, 106, L121111 (2022)

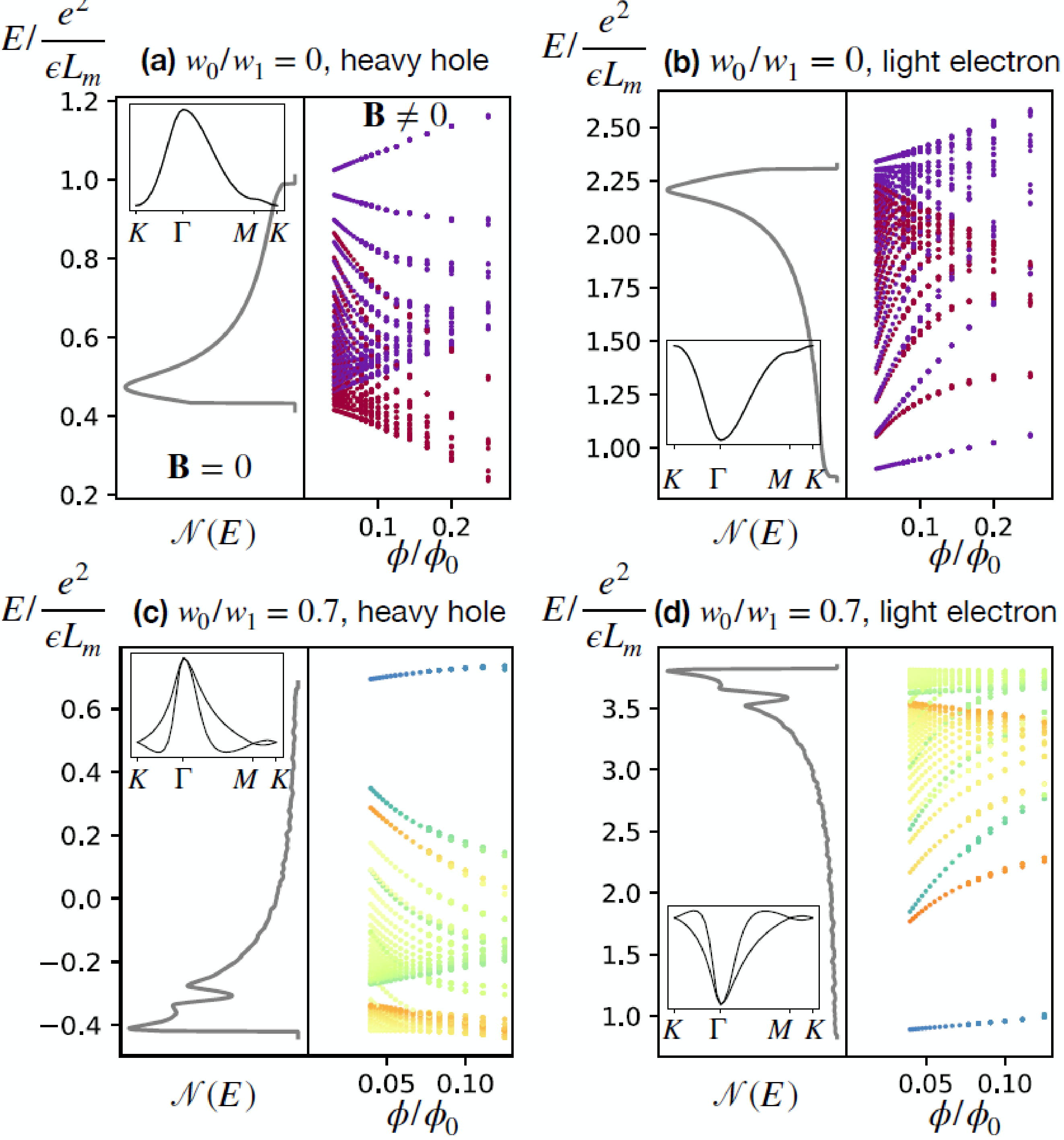

Exact single particle excitation spectrum at ν=2 in the strong coupling limit at small B-field

$$V_{int}\, X|\Omega\rangle =$$
$$\frac{1}{2}\int d\boldsymbol{r}\, d\boldsymbol{r}' V(\boldsymbol{r}-\boldsymbol{r}')\big[\delta\varrho(\boldsymbol{r}),[\delta\varrho(\boldsymbol{r}'),X]\big]|\Omega\rangle$$
$$+\int d\boldsymbol{r}\, d\boldsymbol{r}' V(\boldsymbol{r}-\boldsymbol{r}')[\delta\varrho(\boldsymbol{r}),X\,]\delta\bar{\varrho}(\boldsymbol{r}')|\Omega\rangle$$

- Naturally explains why the Landau fans point away from the CNP

Xiaoyu Wang and OV PRB, 106, L121111 (2022)

Analytic construction of exact zero modes at $\boldsymbol{B} \neq 0$ in the chiral limit: anomaly and the index theorem

$$H_{BM} = \begin{pmatrix} v_F \sigma \cdot (\boldsymbol{p} - \frac{e}{c}\boldsymbol{A}) & T(\boldsymbol{r}) e^{i\boldsymbol{q}_1 \cdot \boldsymbol{r}} \\ e^{-i\boldsymbol{q}_1 \cdot \boldsymbol{r}} T^\dagger(\boldsymbol{r}) & v_F \sigma \cdot (\boldsymbol{p} + \boldsymbol{q}_1 - \frac{e}{c}\boldsymbol{A}) \end{pmatrix}$$

Laughlin gauge: $\boldsymbol{A} = \frac{1}{2} B(-y, x)$

Unlike at $\boldsymbol{B} = 0$, there is no normalizable state on B-sublattice

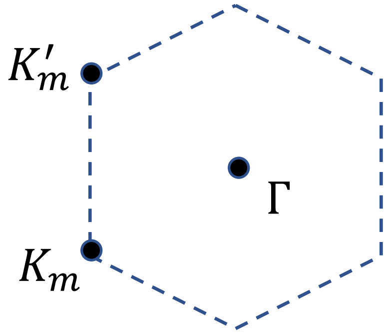

Let $\begin{pmatrix} A_{top} \\ B_{top} \\ A_{bot} \\ B_{bot} \end{pmatrix} \longrightarrow \begin{pmatrix} A_{top} \\ A_{bot} \\ B_{top} \\ B_{bot} \end{pmatrix}$ then $H_{BM} \longrightarrow \begin{pmatrix} 0 & D^\dagger \\ D & 0 \end{pmatrix}$

$$D = \begin{pmatrix} -iv_F \left(2 \frac{\partial}{\partial \bar{z}} + \frac{z}{2\ell_B^2}\right) & w_1 U(\boldsymbol{r}) e^{i\boldsymbol{q}_1 \cdot \boldsymbol{r}} \\ w_1 U(-\boldsymbol{r}) e^{-i\boldsymbol{q}_1 \cdot \boldsymbol{r}} & -iv_F \left(2 \frac{\partial}{\partial \bar{z}} + k_\theta + \frac{z}{2\ell_B^2}\right) \end{pmatrix}$$

$$f(z) e^{-\bar{z}z/4\ell_B^2} \begin{pmatrix} \Psi_{K_m}^{\boldsymbol{B}=0}(\boldsymbol{r}) \\ 0 \end{pmatrix}$$

$$f(z) e^{-\bar{z}z/4\ell_B^2} \begin{pmatrix} \Psi_{K'_m}^{\boldsymbol{B}=0}(\boldsymbol{r}) \\ 0 \end{pmatrix}$$

Popov and Milekhin PRB2021, Sheffer and Stern PRB2021; Xiaoyu Wang and OV PRB, 106, L121111 (2022)

Analytic construction of exact zero modes at $\boldsymbol{B} \neq 0$ in the chiral limit: anomaly and the index theorem

$\boldsymbol{B} = 0$ zero energy states at K_m and K_m' have an opposite parity under $PC_{2y}T$

symmetric gauge: $\boldsymbol{A} = \frac{1}{2}B(-y, x)$

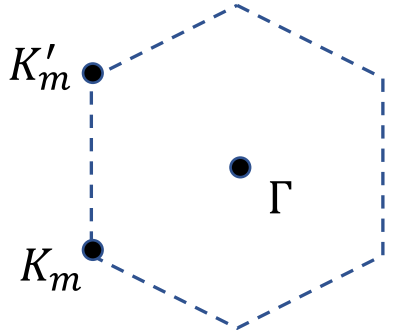

Letting $f(z) = (1, z, z^2, \dots, z^{N-1})$ we therefore prove linear independence of 2Landau levels worth of exact zero energy states living on A sublattice

So for each $k_1 \in (0,1)$ and $k_2 \in (0, \frac{1}{q})$ we have $2p$ zero modes

$$f(z)e^{-\bar{z}z/4\ell_B^2}\begin{pmatrix}\Psi_{K_m}^{B=0}(\boldsymbol{r}) \\ 0\end{pmatrix}$$

$$f(z)e^{-\bar{z}z/4\ell_B^2}\begin{pmatrix}\Psi_{K_m'}^{B=0}(\boldsymbol{r}) \\ 0\end{pmatrix}$$

Because $\{H_{BM}, \sigma_z\} = 0$, by index theorem we must have

$$Tr\langle\sigma_z\rangle = n_+ - n_- = 2p$$

At $\boldsymbol{B} = 0, Tr\langle\sigma_z\rangle = 0$.

Therefore $Tr\langle\sigma_z\rangle$ is *discontinuous* at $\boldsymbol{B} = 0$

Popov and Milekhin PRB2021, Sheffer and Stern PRB2021; Xiaoyu Wang and OV PRB, 106, L121111 (2022)

Exact single particle excitation spectrum at CNP in the strong coupling limit at small B-field at a single k_1, k_2

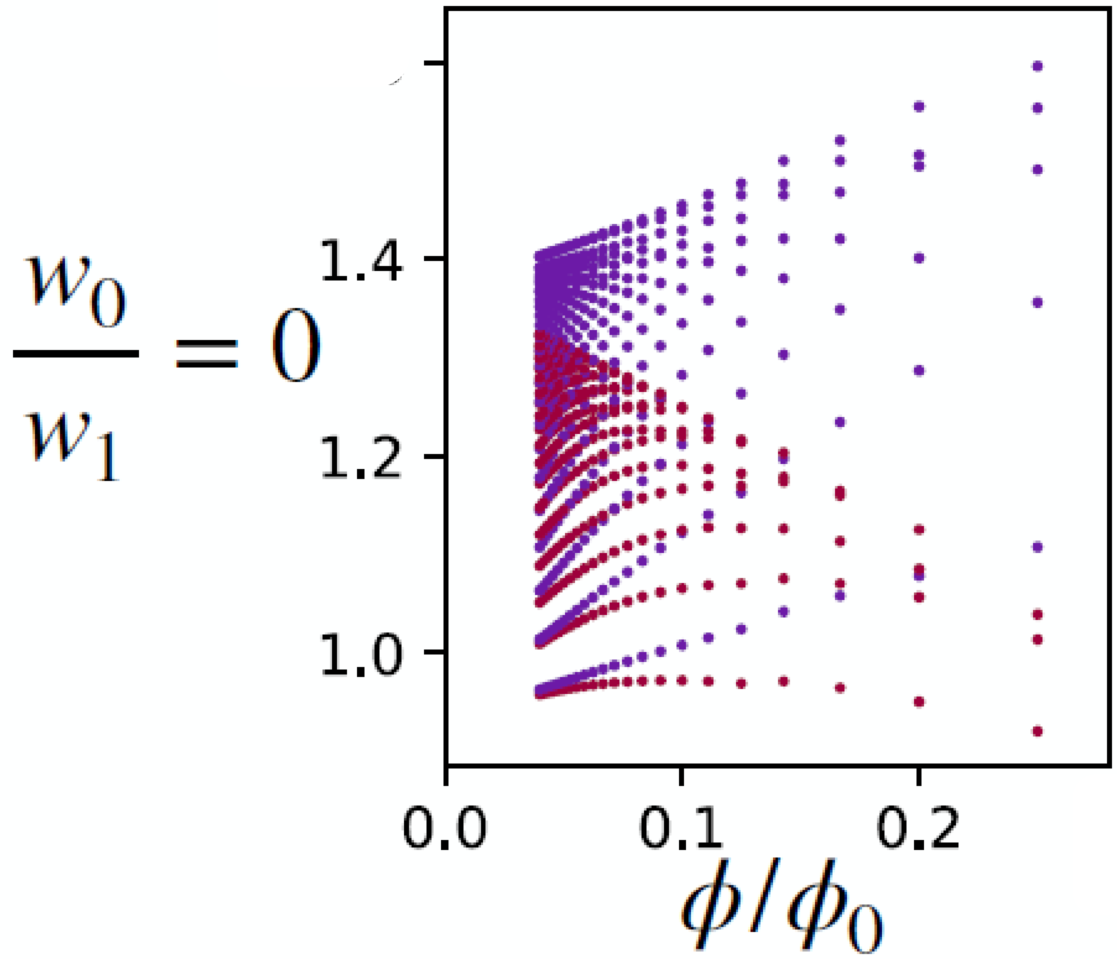

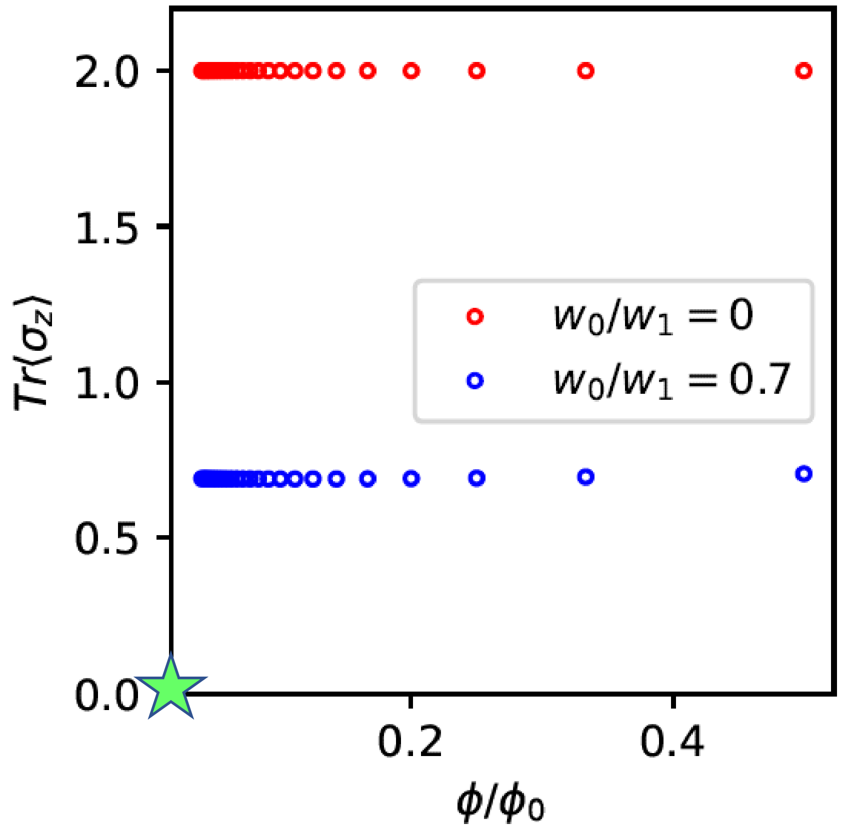

Outlook:

Near degeneracy among many phases implies strong sensitivity terms in the minimal continuum model which were neglected.

This motivates development of a more accurate continuum theory from microscopic model

We can derive the effective continuum model for graphene bilayers by systematically expanding in real space gradients of the slow fermion fields and the atomic displacements allowing for an arbitrary inhomogeneous smooth lattice deformation, including a twist.

- OV and Jian Kang, arXiv:2208.05933
- Jian Kang and OV, arXiv:2208.05953

Lagrangian coordinates:

$$\boldsymbol{X}_{j,S} = \boldsymbol{r}_s + \boldsymbol{u}_{j,S}(\boldsymbol{r}_s)$$

$$\boldsymbol{u}_j(\boldsymbol{r}_s) = \boldsymbol{u}^{\parallel}_{j,S}(\boldsymbol{r}_s) + \boldsymbol{u}^{\perp}_{j,S}(\boldsymbol{r}_s)$$

$$\boldsymbol{r}_s = n_1\boldsymbol{a}_1 + n_2\boldsymbol{a}_2 + \boldsymbol{\tau}_S$$

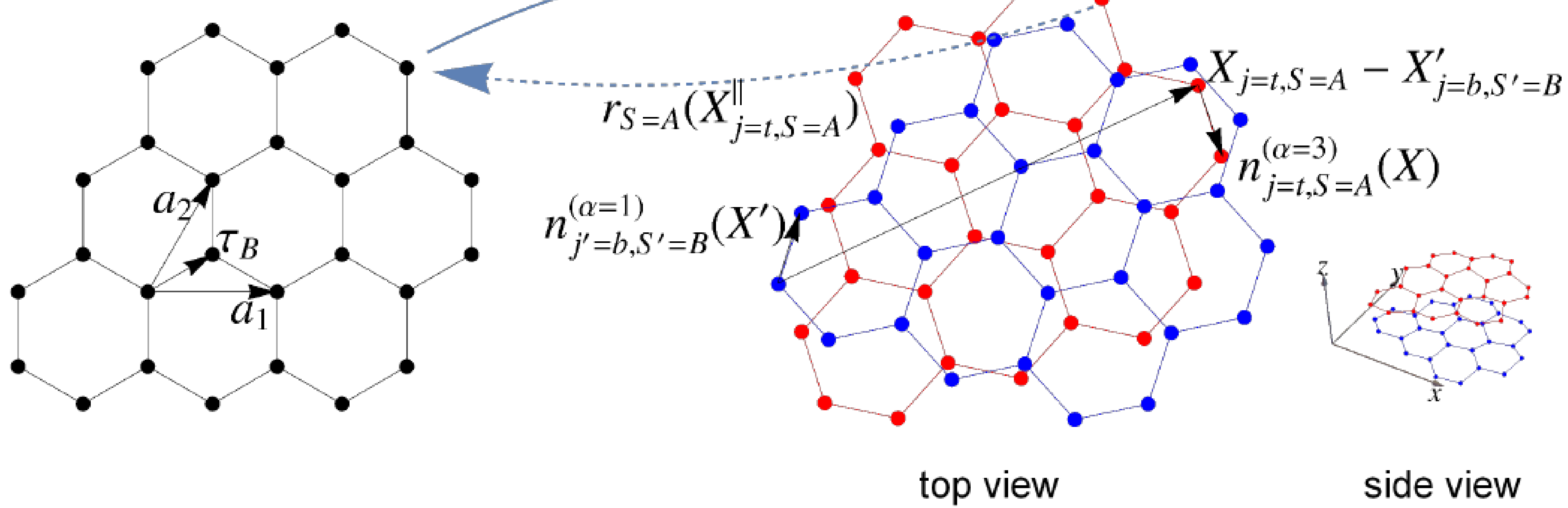

Eulerian coordinates:
(no overhangs ⇒ Monge gauge)

$$\boldsymbol{X}_{j,S} = \boldsymbol{r}_s + \boldsymbol{U}^{\parallel}_{j,S}(\boldsymbol{X}^{\parallel}_{j,S}) + \boldsymbol{U}^{\perp}_{j,S}(\boldsymbol{X}^{\parallel}_{j,S})$$

$$\boldsymbol{r}_s = n_1\boldsymbol{a}_1 + n_2\boldsymbol{a}_2 + \boldsymbol{\tau}_S$$

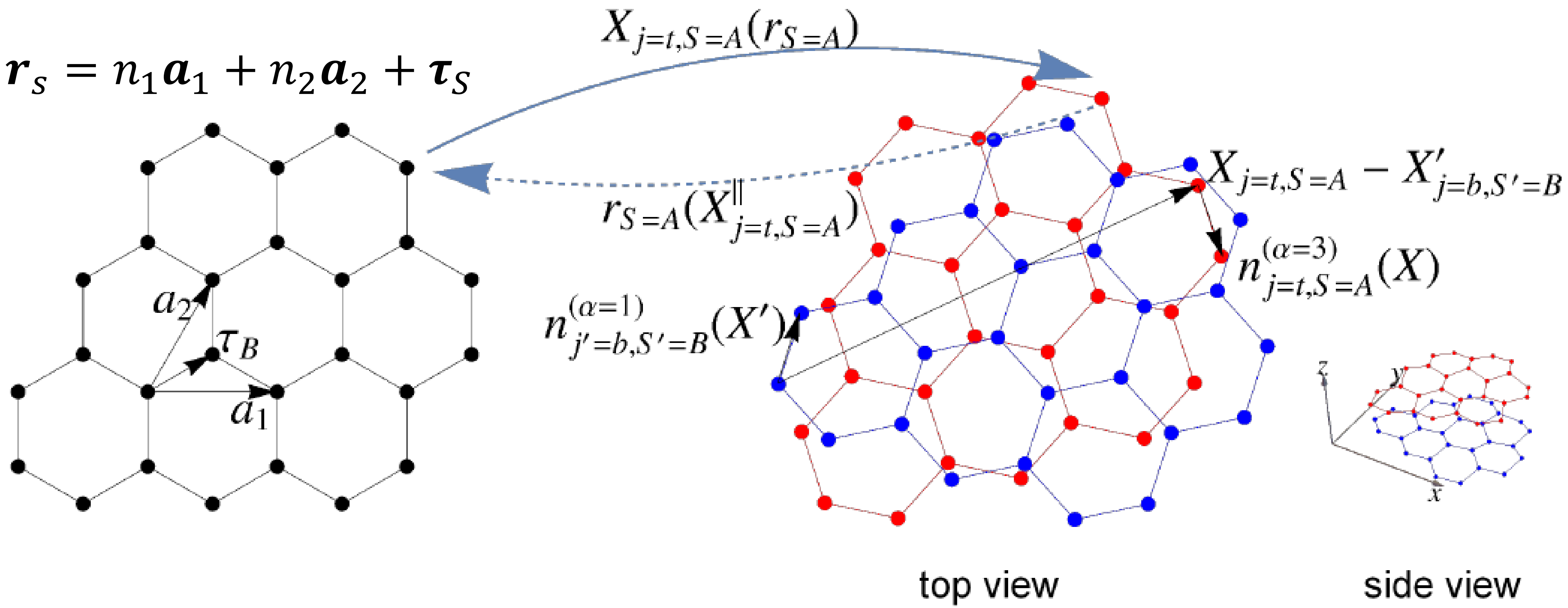

To illustrate the main idea, we assume that the microscopic hopping amplitude t to depend only on the separation of the two carbon atoms, as is the case in Slater-Koster type models.

In general, t depends also on the orientation of this vector relative to the nearest neighbor sites of the atom at $\boldsymbol{X}_{j,S}$ and at $\boldsymbol{X}'_{j',S'}$. Moreover, the general on-site term acquires configuration dependence. We treat this more intricate case in the papers.

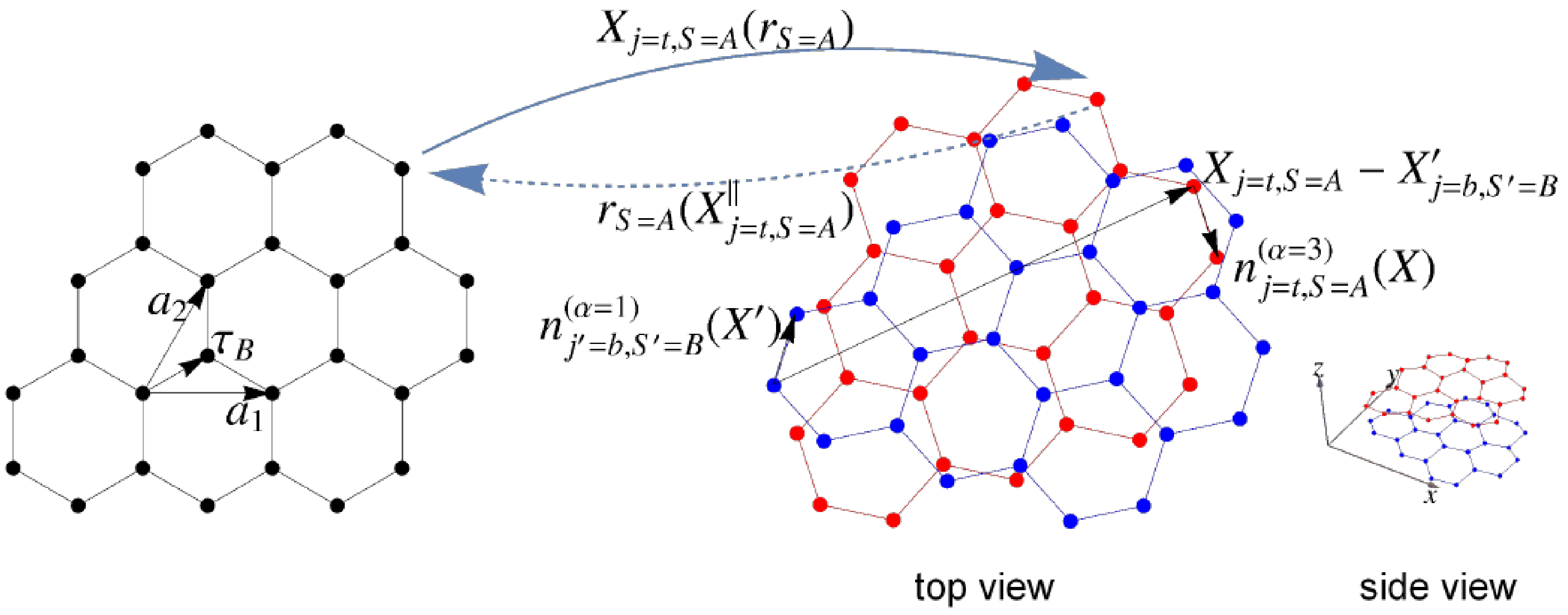

$$H_{tb}^{SK} = \sum_{S,S'} \sum_{j,j'} \sum_{\boldsymbol{r}_S,\boldsymbol{r}'_S} t\left(\boldsymbol{X}_{j,S} - \boldsymbol{X}'_{j',S'}\right) c^{\dagger}_{j,S,\boldsymbol{r}_S} c_{j',S',\boldsymbol{r}'_S}$$

$t(\boldsymbol{X}) = t^*(-\boldsymbol{X})$ because H_{tb}^{SK} is Hermitian

$t(\boldsymbol{X}) = t^*(\boldsymbol{X})$ because H_{tb}^{SK} preserves spinless time reversal symmetry

Example:

$$t(\boldsymbol{X}) = V^0_{pp\pi} e^{-\frac{|\boldsymbol{X}|-a_0}{\Delta}}\left[1 - \left(\frac{\boldsymbol{X}\cdot\hat{z}}{|\boldsymbol{X}|}\right)^2\right] + V^0_{pp\sigma}\, e^{-\frac{|\boldsymbol{X}|-d_0}{\Delta}}\left(\frac{\boldsymbol{X}\cdot\hat{z}}{|\boldsymbol{X}|}\right)^2$$

$V^0_{pp\pi} = -2.7eV$ $V^0_{pp\sigma} = 0.48eV$ $a_0 = |\boldsymbol{\tau}_B| = 0.142nm$ $d_0 = 0.335nm$ $\Delta = 0.319a_0$

G. Trambly de Laissardiere et al, Nano Lett. 10, 804-808 (2010).

$$H_{tb}^{SK} = \sum_{S,S'} \sum_{j,j'} \sum_{\boldsymbol{r}_S,\boldsymbol{r}'_{S'}} \int d^2\boldsymbol{r} \int d^2\boldsymbol{r}'\, \delta(\boldsymbol{r}-\boldsymbol{r}_s)\delta(\boldsymbol{r}'-\boldsymbol{r}'_{S'})t\left(\boldsymbol{r}+\boldsymbol{u}_{j,S}(\boldsymbol{r})-\boldsymbol{r}'-\boldsymbol{u}_{j',S'}(\boldsymbol{r}')\right) c^\dagger_{j,S,\boldsymbol{r}} c_{j',S',\boldsymbol{r}'}$$

$$\sum_{\boldsymbol{r}_S} \delta(\boldsymbol{r}-\boldsymbol{r}_s) = \frac{1}{|\boldsymbol{a}_1 \times \boldsymbol{a}_2|} \sum_{\boldsymbol{G}} e^{i\boldsymbol{G}\cdot(\boldsymbol{r}-\boldsymbol{\tau}_S)}; \quad \boldsymbol{G} = 2\pi(m_1\boldsymbol{a}_2 - m_2\boldsymbol{a}_1) \times \frac{\hat{z}}{|\boldsymbol{a}_1 \times \boldsymbol{a}_2|}$$

The physically important states come from the vicinity of the Dirac points. Therefore, we can decompose the fermion fields into two slowly spatially varying fields ψ and ϕ multiplied by the fast spatially varying functions from the valley $\boldsymbol{K} = 4\pi\boldsymbol{a}_1/(3a^2)$ and $\boldsymbol{K}' = -\boldsymbol{K}$.

$$\frac{1}{\sqrt{|\boldsymbol{a}_1 \times \boldsymbol{a}_2|}} c_{j,S,\boldsymbol{r}} \cong e^{i\boldsymbol{K}\cdot\boldsymbol{r}}\psi_{j,S}(\boldsymbol{r}) + e^{-i\boldsymbol{K}\cdot\boldsymbol{r}}\phi_{j,S}(\boldsymbol{r})$$

$$\left\{\psi_{j,S}(\boldsymbol{r}), \psi^\dagger_{j',S'}(\boldsymbol{r}')\right\} = \left\{\phi_{j,S}(\boldsymbol{r}), \phi^\dagger_{j',S'}(\boldsymbol{r}')\right\} = \delta_{j,j'}\delta_{S,S'}\delta(\boldsymbol{r}-\boldsymbol{r}')$$

$$H^{\boldsymbol{K}}_{SK,eff} = \frac{1}{|\boldsymbol{a}_1 \times \boldsymbol{a}_2|}\sum_{S,S'}\sum_{j,j'}\sum_{\boldsymbol{G},\boldsymbol{G}'}\int d^2\boldsymbol{r}\int d^2\boldsymbol{r}'\, e^{i\boldsymbol{G}\cdot(\boldsymbol{r}-\boldsymbol{\tau}_S)} e^{-i\boldsymbol{G}'\cdot(\boldsymbol{r}'-\boldsymbol{\tau}_{S'})} t\left(\overset{\boldsymbol{X}}{\boldsymbol{r}+\boldsymbol{u}_{j,S}(\boldsymbol{r})} - \boldsymbol{r}' - \boldsymbol{u}_{j',S'}(\boldsymbol{r}')\right) e^{-i\boldsymbol{K}\cdot(\boldsymbol{r}-\boldsymbol{r}')}\psi^{\dagger}_{j,S}(\boldsymbol{r})\psi_{j',S'}(\boldsymbol{r}')$$

short ranged

$$\Psi_{j,S}(\boldsymbol{X}^{\|}) = \sqrt{\left|J\left(\frac{\partial \boldsymbol{r}}{\partial \boldsymbol{X}^{\|}}\right)\right|}\,\psi_{j,S}(\boldsymbol{r}) \qquad \left\{\Psi_{j,S}(\boldsymbol{X}^{\|}), \Psi^{\dagger}_{j',S'}(\boldsymbol{X}'^{\|})\right\} = \delta_{j,j'}\delta_{S,S'}\delta\left(\boldsymbol{X}^{\|} - \boldsymbol{X}'^{\|}\right)$$

$$H^{\boldsymbol{K}}_{SK,eff} = \frac{1}{|\boldsymbol{a}_1 \times \boldsymbol{a}_2|}\sum_{S,S'}\sum_{j,j'}\sum_{\boldsymbol{G},\boldsymbol{G}'} e^{-i\left(\boldsymbol{G}\cdot\boldsymbol{\tau}_S - \boldsymbol{G}'\cdot\boldsymbol{\tau}_{S'}\right)}\int d^2\boldsymbol{X}^{\|}\sqrt{\left|J\left(\frac{\partial \boldsymbol{r}}{\partial \boldsymbol{X}^{\|}}\right)\right|}\int d^2\boldsymbol{X}'^{\|}\sqrt{\left|J\left(\frac{\partial \boldsymbol{r}'}{\partial \boldsymbol{X}'^{\|}}\right)\right|}\, e^{-i(\boldsymbol{G}-\boldsymbol{K})\cdot\boldsymbol{U}^{\|}_{j,S}(\boldsymbol{X}^{\|})} e^{i(\boldsymbol{G}'-\boldsymbol{K})\cdot\boldsymbol{U}^{\|}_{j',S'}(\boldsymbol{X}'^{\|})} t\Big(\boldsymbol{X}^{\|} + \boldsymbol{U}^{\perp}_{j,S}(\boldsymbol{X}^{\|}) - \boldsymbol{X}'^{\|} - \boldsymbol{U}^{\perp}_{j',S'}(\boldsymbol{X}'^{\|})\Big) e^{i(\boldsymbol{G}\cdot\boldsymbol{X}^{\|} - \boldsymbol{G}'\cdot\boldsymbol{X}'^{\|})} e^{-i\boldsymbol{K}\cdot(\boldsymbol{X}^{\|}-\boldsymbol{X}'^{\|})}\Psi^{\dagger}_{j,S}(\boldsymbol{X}^{\|})\Psi_{j',S'}(\boldsymbol{X}'^{\|})$$

$$H_{SK,eff}^{\boldsymbol{K}} =$$

$$\frac{1}{|\boldsymbol{a}_1 \times \boldsymbol{a}_2|} \sum_{S,S'} \sum_{j,j'} \sum_{\boldsymbol{G},\boldsymbol{G}'} e^{-i(\boldsymbol{G}\cdot\boldsymbol{\tau}_S - \boldsymbol{G}'\cdot\boldsymbol{\tau}_{S'})} \int d^2\boldsymbol{X}^{\parallel} \sqrt{\left| J\left(\frac{\partial \boldsymbol{r}}{\partial \boldsymbol{X}^{\parallel}}\right)\right|} \int d^2\boldsymbol{X}'^{\parallel} \sqrt{\left| J\left(\frac{\partial \boldsymbol{r}'}{\partial \boldsymbol{X}'^{\parallel}}\right)\right|} e^{-i(\boldsymbol{G}-\boldsymbol{K})\cdot\boldsymbol{U}^{\parallel}_{j,S}(\boldsymbol{X}^{\parallel})} e^{i(\boldsymbol{G}'-\boldsymbol{K})\cdot\boldsymbol{U}^{\parallel}_{j',S'}(\boldsymbol{X}'^{\parallel})} t\Big(\boldsymbol{X}^{\parallel}$$

$$+ \boldsymbol{U}^{\perp}_{j,S}(\boldsymbol{X}^{\parallel}) - \boldsymbol{X}'^{\parallel} - \boldsymbol{U}^{\perp}_{j',S'}(\boldsymbol{X}'^{\parallel})\Big) e^{i(\boldsymbol{G}\cdot\boldsymbol{X}^{\parallel} - \boldsymbol{G}'\cdot\boldsymbol{X}'^{\parallel})} e^{-i\boldsymbol{K}\cdot(\boldsymbol{X}^{\parallel} - \boldsymbol{X}'^{\parallel})} \Psi^{\dagger}_{j,S}(\boldsymbol{X}^{\parallel}) \Psi_{j',S'}(\boldsymbol{X}'^{\parallel})$$

$$\boldsymbol{x} = \frac{1}{2}\left(\boldsymbol{X}^{\parallel} + \boldsymbol{X}'^{\parallel}\right) \qquad\qquad \boldsymbol{y} = \boldsymbol{X}^{\parallel} - \boldsymbol{X}'^{\parallel}$$

$$e^{i(\boldsymbol{G}\cdot\boldsymbol{X}^{\parallel} - \boldsymbol{G}'\cdot\boldsymbol{X}'^{\parallel})} = e^{i(\boldsymbol{G}-\boldsymbol{G}')\cdot\boldsymbol{x}} e^{i(\boldsymbol{G}+\boldsymbol{G}')\cdot\boldsymbol{y}/2}$$

Oscillates strongly unless $\boldsymbol{G} = \boldsymbol{G}'$. All other factors a slow functions of $\boldsymbol{x}$

$$\boldsymbol{U}^{\parallel}_{j,S}(\boldsymbol{X}^{\parallel}) = \boldsymbol{U}^{\parallel}_{j,S}\left(\boldsymbol{x} + \frac{1}{2}\boldsymbol{y}\right) \simeq \boldsymbol{U}^{\parallel}_{j,S}(\boldsymbol{x}) + \frac{1}{2}\boldsymbol{y}\cdot\partial\boldsymbol{U}^{\parallel}_{j,S}(\boldsymbol{x}) + \cdots$$

$$\frac{1}{|\boldsymbol{a}_1 \times \boldsymbol{a}_2|}$$

$$\sqrt{\left|J\left(\frac{\partial \boldsymbol{r}}{\partial \boldsymbol{X}^{\parallel}}\right)\right|}$$

$$H^{\mathbf{K}}_{SK,eff} \simeq \frac{1}{A_{mlg}} \sum_{S,S'} \sum_{jj'} \sum_{\boldsymbol{G}} e^{i\boldsymbol{G}\cdot(\boldsymbol{\tau}_S - \boldsymbol{\tau}_{S'})} \int \mathrm{d}^2\boldsymbol{x}\, \mathcal{J}_{j,S}(\boldsymbol{x}) \mathcal{J}_{j',S'}(\boldsymbol{x}) e^{i(\boldsymbol{G}+\boldsymbol{K})\cdot\left(\boldsymbol{U}^{\parallel}_{j,S}(\boldsymbol{x}) - \boldsymbol{U}^{\parallel}_{j',S'}(\boldsymbol{x})\right)}$$

$$\int \mathrm{d}^2\boldsymbol{y}\, e^{-i(\boldsymbol{G}+\boldsymbol{K})\cdot\boldsymbol{y}} e^{i\frac{\boldsymbol{y}}{2}\cdot\nabla_{\boldsymbol{x}}\left(\boldsymbol{U}^{\parallel}_{j,S}(\boldsymbol{x}) + \boldsymbol{U}^{\parallel}_{j',S'}(\boldsymbol{x})\right)\cdot(\boldsymbol{G}+\boldsymbol{K})} t\left[\boldsymbol{y} + \boldsymbol{U}^{\perp}_{j,S}(\boldsymbol{x}) - \boldsymbol{U}^{\perp}_{j',S'}(\boldsymbol{x})\right]$$

$$\times \left[\Psi^{\dagger}_{j,S}(\boldsymbol{x})\Psi_{j',S'}(\boldsymbol{x}) + \frac{\boldsymbol{y}}{2}\cdot\left(\left(\nabla_{\boldsymbol{x}}\Psi^{\dagger}_{j,S}(\boldsymbol{x})\right)\Psi_{j',S'}(\boldsymbol{x}) - \Psi^{\dagger}_{j,S}(\boldsymbol{x})\nabla_{\boldsymbol{x}}\Psi_{j',S'}(\boldsymbol{x})\right)\right].$$

- OV and Jian Kang, arXiv:2208.05933
- Jian Kang and OV, arXiv:2208.05953

$$H_{intra}^{(0)} = \int \mathrm{d}^2x \sum_{j=t,b} \sum_{SS'} \Psi_{j,S}^{\dagger}(\boldsymbol{x}) \Big\{ \mu\delta_{SS'} + v_F \bar{\boldsymbol{\sigma}}_{SS'} \cdot \left(\boldsymbol{p}^{(j)} + \gamma \mathcal{A}^{(j)}(\boldsymbol{x}) \right) + \beta_0 \boldsymbol{p}^2 \delta_{SS'} + \frac{C_0}{2} \left(\boldsymbol{p} \cdot \mathcal{A}(\boldsymbol{x}) + \mathcal{A}(\boldsymbol{x}) \cdot \boldsymbol{p} \right) \delta_{SS'}$$

$$+ \beta_1 \left((p_x^2 - p_y^2)\sigma_1 + 2p_x p_y \sigma_2 \right)_{SS'} + \frac{1}{2} \sum_{\mu} \left(p_\mu \xi_{\mu,SS'}(\boldsymbol{x}) + \xi_{\mu,SS'}(\boldsymbol{x}) p_\mu \right) \Big\} \Psi_{j,S}(\boldsymbol{x}),$$

$$H_{inter} = \sum_{SS'} \int \mathrm{d}^2x \Psi_{t,S}^{\dagger}(\boldsymbol{x}) \left(T_{SS'}(\boldsymbol{x}) + \frac{1}{2} \left\{ \boldsymbol{p}, \boldsymbol{\Lambda}_{SS'}(\boldsymbol{x}) \right\} \right) \Psi_{b,S'}(\boldsymbol{x}) + h.c..$$

- OV and Jian Kang, arXiv:2208.05933
- Jian Kang and OV, arXiv:2208.05953

Example: rigid twist

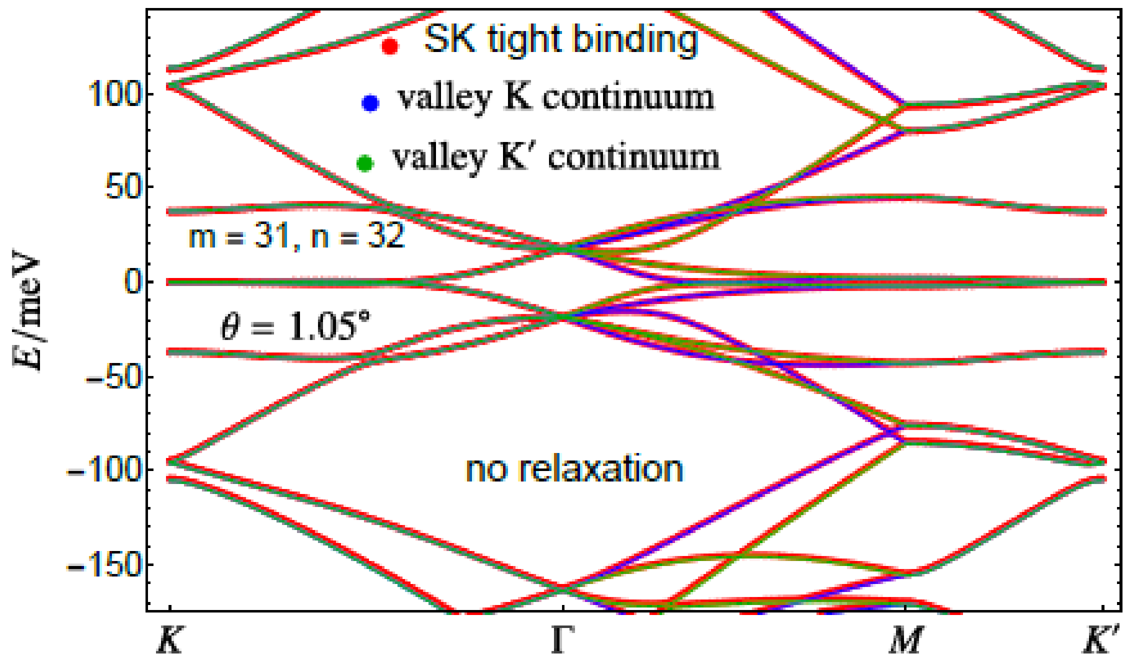

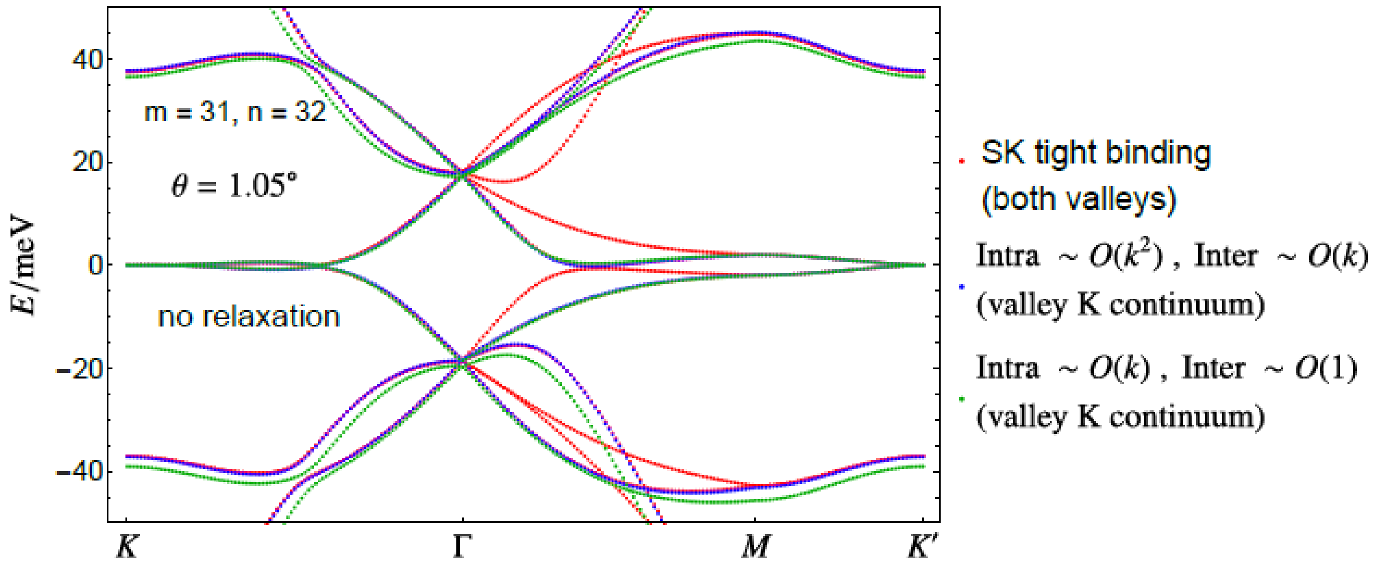

Beyond rigid twist

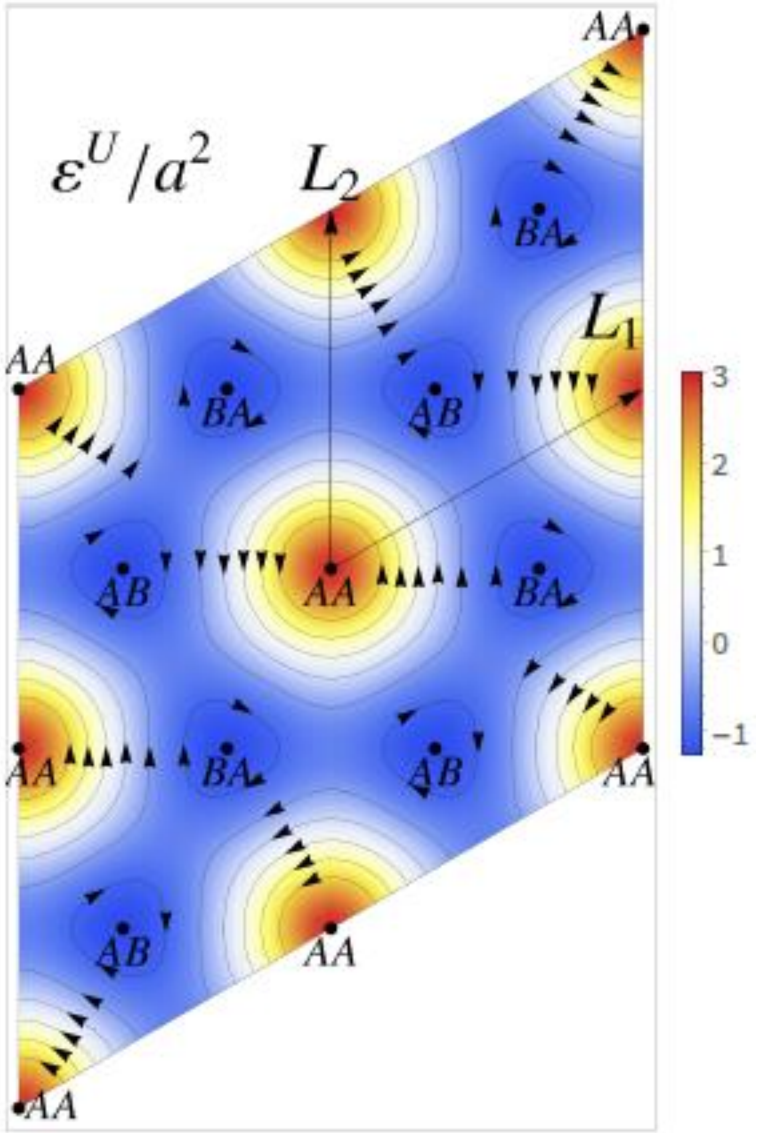

$$\delta \boldsymbol{U}(\boldsymbol{x}) = \boldsymbol{\nabla}\varphi^U(\boldsymbol{x}) + \boldsymbol{\nabla} \times \left(\hat{\boldsymbol{z}}\varepsilon^U(\boldsymbol{x})\right)$$